MULTILEVEL MEASUREMENTS OF SURFACE TEMPERATURE OVER UNDULATING TERRAIN PLANTED TO BARLEY

R. J. Reginato[1/], J. P. Millard[2/], J. L. Hatfield[3/], and R. D. Jackson[1/]
(Principal Investigator)

(E82-10245) MULTILEVEL MEASUREMENTS OF SURFACE TEMPERATURE OVER UNDULATING TERRAIN PLANTED TO BARLEY Final Report, 1 Nov. 1977 - 31 Oct. 1980 (NASA) 74 p HC A04/MF A01 CSCL 04B G3/43

N82-24523

Unclas 00245

1/ U. S. Water Conservation Laboratory, SEA/AR, USDA
4331 East Broadway Road
Phoenix, AZ 85040

2/ Code 240-6, NASA/Ames Research Center
Moffett Field, CA 94035

3/ Dept. of Land, Air, and Water Resources
University of California
Davis, CA 95616

March 1981
Type III Final Report. Contract No. S0255B

Prepared for

NASA/Goddard Space Flight Center
Greenbelt, MD 20771

TECHNICAL REPORT STANDARD TITLE PAGE

1. Report No.	2. Government Accession No.	3. Recipient's Catalog No.

4. Title and Subtitle
Multilevel measurements of surface temperature over undulating terrain planted to barley

5. Report Date
March 1981

6. Performing Organization Code

7. Author(s)
R.J.Reginato, J.P.Millard, J.L.Hatfield, R.D.Jackson

8. Performing Organization Report No.

9. Performing Organization Name and Address
U. S. Water Conservation Laboratory
4331 East Broadway Road
Phoenix, AZ 85040

10. Work Unit No.

11. Contract or Grant No.
S-40255B

13. Type of Report and Period Covered
Type III Final Report
1 Nov 77 to 31 Oct 80

12. Sponsoring Agency Name and Address
R. Stonesifer
Goddard Space Flight Center
Greenbelt, MD 20771

14. Sponsoring Agency Code

15. Supplementary Notes Prepared in cooperation with
J. P. Millard
NASA/Ames Research Center
Moffett Field, CA 94035
and
J. L. Hatfield
Dept. of Land, Air, and Water Res.
Univ. of California, Davis, CA 95616

16. Abstract A ground and aircraft program was conducted to extend ground-based methods for measuring soil moisture and crop water stress to aircraft and satellite altitudes. A 260ha agricultural field in California was used over the 1977-78 growing season. Delay of the launch of the HCMM and unexpected heavy rainfall made it impossible to accomplish all of the original objectives in the detail desired. For cloud-free days ground-based temperature measurements over bare soil were related to soil moisture content. Water stress resulted from too much water, not from lack of it, as was expected. A theoretical explanation of the canopy-air temperature difference as affected by vapor pressure deficit and net radiation was developed. This analysis shows why surface temperatures delineate crop water stress under conditions of low humidity, but not under high humidity conditions. Multilevel temperatures acquired from the ground, low and high altitude aircraft and the HCMM spacecraft were compared for two day and one night overpasses. The U-2 and low altitude temperatures were within 0.5°C. The HCMM data were analyzed using both the pre- and post-launch calibrations, with the former being considerably closer in agreement with the aircraft data than the latter.

17. Key Words (Selected by Author(s))
canopy temperature, soil moisture, multilevel measurements, barley, undulating terrain, yield prediction

18. Distribution Statement

19. Security Classif. (of this report)	20. Security Classif. (of this page)	21. No. of Pages	22. Price*

*For sale by the Clearinghouse for Federal Scientific and Technical Information, Springfield, Virginia 22151.

TABLE OF CONTENTS

ABSTRACT

Results from ground-based experiments using hand-held infrared radiometers had shown that remotely sensed surface temperatures could be used to estimate surface temperatures of bare soil and to estimate crop water stress. An intensive ground and aircraft program was planned, in conjunction with the HCMM, to extend the ground-based methods to aircraft and satellite altitudes. The HCMM was scheduled for a one year mission beginning with launch in October 1977. A large agricultural field was selected in California (to be near the aircraft base and a university) as the site for the experiment. The growing season 1977-78 was to be during the one year life of the HCMM. After the ground and aircraft program had begun, the launch date was delayed. This delay and the unexpected heavy rainfall made it impossible to accomplish the original objectives in the detail desired. However, at three times late in the season, ground, low- and high-altitude aircraft, and HCMM spacecraft data were obtained. Comparison of the multilevel acquired temperatures indicated that the soil moisture and yield prediction techniques developed on the basis of data acquired on the ground can be extended to satellite altitudes, providing that problems of registration and accounting for atmospheric effects are adequately addressed.

The plant growth and development data acquired over undulating terrain provided a data set that pointed out problems associated with interpreting remotely sensed plant temperatures under different slopes and aspects. The south-facing slopes had the highest yields. The low areas were poorly drained and consequently had low yields. Weeds grew well in

the low areas and the vegetation temperatures were about the same as for the better sites. Yield models using stress-degree-day inputs did not account for the weeds and hence overpredicted yields. Had the experiment been conducted in a dry year, the low areas would probably been the highest yielding areas with the south-facing slopes yielding the lowest because of a lack of water.

For cloud-free days, ground-based temperature measurements over bare soil were related to soil moisture content. Due to the abnormally high rainfall, water stress resulted from too much water, not from the lack of it as was expected.

A theory was developed to explain how vapor-pressure deficit and net radiation affect the difference in temperature between the canopy and the air. This analysis showed why canopy temperatures can delineate crop water stress under conditions of low humidity but not under high humidity. This development could be used to predict when or where stress conditions may or may not be detectable using thermal sensors on spacecraft.

Ground and aircraft derived temperatures were registered in space and time for seven flights. The spatial registration was within a 5-pixel grid. The relation between ground and aircraft data had an intercept of near 0 and a slope of 1.07, indicating that the aircraft temperatures were slightly warmer than ground temperatures at higher ambient temperatures. The same relation held when ground temperatures from 16 sites were averaged and compared with aircraft temperatures integrated to give one value for the entire 260 ha field. This result indicates that methods

derived from ground-based experiments for estimating soil moisture and crop water stress are adaptable to aircraft programs.

To gain an insight into appropriate pixel sizes needed for undulating terrain, the 2 m x 2 m pixels from one aircraft data set were averaged to produce 200 m x 200 m, 400 m x 400 m, and 800 m x 800 m pixels. When one high altitude data set was included, it was found that pixel sizes ranging from 70 m x 70 m to 800 m x 800 m yielded essentially the same temperature information for the entire barley field. For surveying large areas of grain, high resolution is not necessary, except for the problem of the location of specific sites. It was extremely difficult to locate the experimental field, which was about 9 HCMM pixels in size.

Multilevel temperatures, acquired from the ground, low and high altitude aircraft, and the HCMM spacecraft were compared for two day and one night overpasses. The U-2 and low altitude temperatures differed by less than 0.5°C. The HCMM data were analyzed using both the pre- and post-launch calibrations. The pre-launch calibration temperatures were considerably closer to the aircraft data than the post-launch calibrated temperatures. For the pre-launch calibrated data, HCMM temperatures were higher at night and lower during the day when compared to the aircraft data. These differences may result from the HCMM radiometer calibration or from the inability to account exactly for atmospheric effects.

ACKNOWLEDGEMENTS

Many people contributed to the project reported here. Ronald S. Seay of the U. S. Water Conservation Laboratory worked diligently with Reginato to obtain the ground data. He independently made periodic assessment of the entomological status of the barley throughout the growing season. At NASA/Ames, R. C. Goettelman and M. J. LeRoy worked with Millard to collect, analyze, and present the aircraft-derived data. They also processed the HCMM tapes and prepared the imagery. At U.C. Davis, a number of Hatfield's graduate students provided considerable expertise. Carol Whitman analyzed the plant samples and prepared an outstanding M.S. thesis on various aspects of plant growth on undulating terrain. Graham Walker, Larry Hipps, and Mike Sully provided essential advice and effort. Thanks are also due to John Price, Locke Stuart, and Richard Stonesifer of the Goddard Space Flight Center for their help throughout the course of this project.

We offer a special thanks to Karl and John Giguire, the owner-operators of the farm that we used as an experimental area. They were most cooperative and supportive, and showed an active interest in our project.

LIST OF ILLUSTRATIONS

LIST OF TABLES

INTRODUCTION

In the early 1970's soil physics research at the U. S. Water Conservation Laboratory focused on the diurnal soil moisture changes occurring in the surface layer (≈ 10 cm) of field soils. These changes, driven by moisture and temperature gradients within the soil and by meterological factors above the soil, required intensive field experiments to document. Although the original objectives of the experiments were to provide data for testing theories of simultaneous flow of heat and moisture in soil, they proved to be a comprehensive data base for testing soil moisture models used in remote sensing, and for actually relating temperature data that could be obtained remotely, to soil moisture. Some of these data were used by NASA to help show the possibilities of the HCMM satellite to estimate soil moisture.

After developing the data to the point that it appeared feasible to estimate soil moisture (in the first few cm of the surface) from remotely sensed surface temperatures (both ground and aircraft based) we began to look at the possibilities of using surface temperatures to evaluate crop water stress and thus indirectly measure soil moisture. While these ideas were in their infancy, the opportunity to propose an HCMM experiment arose. We felt that full utilization of our work on soil moisture would not evolve until it was demonstrated that the methods, or modifications of them, could be used with spacecraft data. Furthermore, with our emerging hopes that similar methods could be developed for detecting crop water stress, we felt that a satellite with a thermal sensor aboard,

could become a useful tool for assessing regional crop water status as well as soil moisture of relatively bare fields. Thus, our HCMM proposal dealt largely with estimating soil moisture with crop water stress being a minor part. Our research on crop water stress continued at a rapid rate and, after our proposal was accepted and detailed planning for the experiments proceeded, it was evident that crop water stress would be the major thrust of our experiments. Specific objectives given in the statement of work (written sometime after the proposal was accepted) were:

1. Evaluate the feasibility of monitoring soil moisture at a selected bare-soil test site on a repetitive basis by thermal methods.
2. Evaluate the feasibility of monitoring plant water stress at a plant-canopied test site by measuring plant and air temperatures.
3. Evaluate the feasibility of monitoring wheat biostages at a selected test site by albedo and plant temperature methods.
4. Evaluate the feasibility of estimating wheat yields at a selected test site by albedo and plant temperature methods.

The long-range objective was to develop techniques for monitoring soil moisture, plant water stress, and crop yields on a global basis.

The proposal was accepted in March 1976 and detailed planning for the ground and aircraft experiments began immediately. Launch of the HCMM was scheduled for October, 1977, with a planned operating life of one year. We were faced with the problem of conducting ground experiments over a large enough site that would be covered by a minimum of 9 pixels in an HCMM image. An intensive low altitude (≈ 1 km) aircraft

program was designed to interface the ground and spacecraft data, and to provide data to calibrate the spacecraft sensor if necessary. The aircraft program was made possible by NASA/Ames Research Center. An excellent working relationship had developed between the NASA group and the U. S. Water Conservation Laboratory during earlier cooperative experiments.

We chose a site west of Sacramento, CA (38° 49'N, 121° 59'W) that included about 260 ha of nonirrigated wheat. The topography of the field was varied so it was expected that areas would be stressed and other areas would have adequate water. California was undergoing a severe drought during this time (1976-1977). Our plans were to begin the experiment in the fall of 1977 and carry it through the growing season. Planting was scheduled for the normal November-December time, in close conjunction with the scheduled October launch of the HCMM.

In August 1977, we transferred a scientist and a technician to Davis, CA, for a one-year period. They made the final site selection and gathered the equipment necessary for the intensive ground measurements that were required. (Pre-dawn and afternoon HCMM time IR temperature measurements were to be made at 16 locations every day during the growing season.) About this time word reached us that the launch date had slipped a few weeks. Due to the severity of the drought, the farm owner decided to plant barley instead of wheat because of its greater drought tolerance. Planting began on schedule. When about half of the 260 ha were planted, the drought broke. Rains delayed planting and caused some

flooding in the lower areas. Above average rainfall occurred during the entire season, and further delays in the launch of the HCMM were announced.

We proceeded with the ground measurements and the aircraft program. (The aircraft was grounded for repairs during April.) The HCMM, launched on 26 April 1978, took its first data while the site was being harvested. Multistage data (ground, aircraft, spacecraft) were obtained for three satellite overpasses.

The 670 mm of rain during the period November 1977 through April 1978 were exceeded in this area only once since rainfall records have been kept. The soil was so wet that stress due to too much water was observed, instead of due to lack of water as we expected. Along with the rain, cloudy weather prevailed much of the time, making the interpretation of temperature data difficult. The abnormal weather and the delayed launch precluded the fulfillment of several objectives. In spite of the problems encountered, some results of interest were obtained.

EXPERIMENTAL PREPARATIONS AND PROCEDURES

Site Selection

The criteria developed for site selection were:

1. Terrain typical of major grain-growing areas.
2. Good farmer cooperation.
3. At least 250 ha area of land, nearly square, all planted to the same crop.
4. Climate favorable for dryland grain production.

5. An area where there was a possibility of some crop water stress developing because of land relief and/or previous climatic drought history.
6. Close to NASA/Ames Research Center in order to minimize flight times for the aircraft program.
7. Close to a University in order to obtain essential personnel, space, services, and equipment.

The location selected was a 260 ha field near Dunnigan, 35 miles northwest of the University of California, Davis, Yolo County, California. The field encompassed parts of sections 9, 15, and 16 of Range 1 West, Township 11 North; coordinates 38° 49'N, 121° 59' West. The terrain ranged from flat to 45% slopes. A narrow unpaved dirt road ran through the center of the field.

The cropping history of the field was wheat or barley, with alternate years fallow. California had undergone a second year of drought and dry conditions were predicted through 1977. The owner-operators had previously cooperated with the University of California on other experiments. They agreed to perform all normal cultural operations, and we, in turn, agreed to reimburse them for damages caused by our experimental procedures.

Experimental Sites

Sixteen sites were chosen within the 260 ha field at which the ground measurements would be made (figure 1). The letter R designates remote sites which were not fully instrumental (with the exception of R1 near headquarters). The main fully instrumented sites were located near

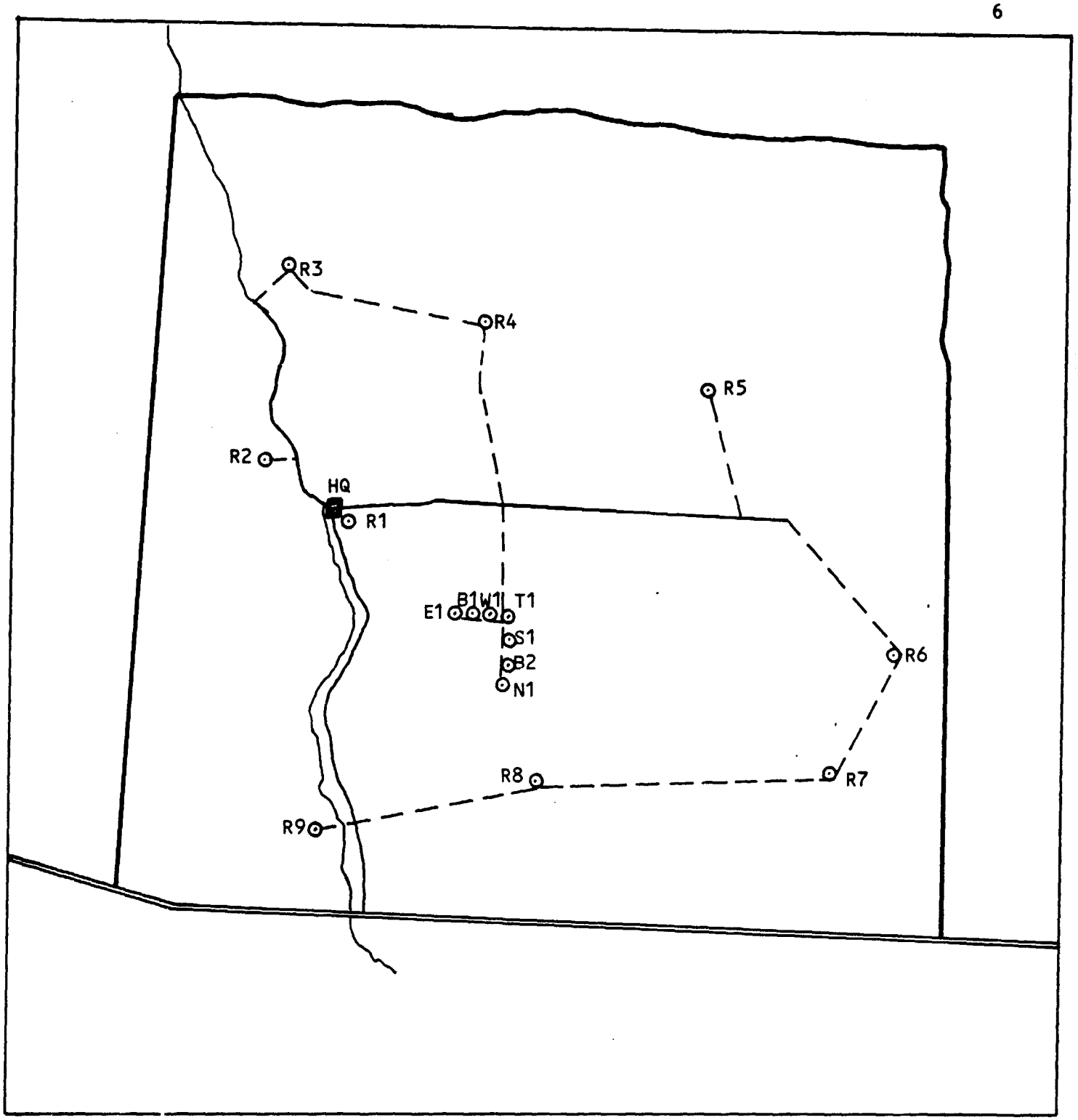

Figure 1. Diagram of the approximately 260ha agricultural field showing the 16 measurement sites, roads, and paths for reaching the sites.

the center of the field. The location symbols were; T = top of knoll, B = bottom of gully, E = east-facing slope, W = west-facing slope, S = south-facing slope, and N = north facing slope. An aerial photo taken on 10 March 1978 is shown in figure 2, and with the aid of figure 1, the 16 sites can be located on the photo. The paths used to go from one site to another are readily detectable in the photo. Also the rolling nature of the terrain, the drainage patterns, and the differing plant density can be discerned. A description of the slope, aspect, and planting row direction for each site is given in Table 1. The 16 sites were divided into two slope categories: 0-10% and >10%. Similarly, aspects (directions in which the slopes faced) in the four cardinal directions (north, east, south, and west) were selected within each slope class.

In order to instrument several sites for intensive measurements, seven sites were located such that two transects (east-west and north-south) that intersected at right angles were formed. This was called the main site.

An effort was made to space the 16 sites throughout the entire field, so the comparisons could be made between ground, aircraft, and satellite data. However, time constraints dictated that the sites be located so that measurements on all could be made within a 30-minute period. The final site selection, as shown in Figure 1, came close to meeting these requirements. The path connecting the sites was 3.5 miles long and traversed slopes from 0 to 36%. Each site consisted of a 15 m square target area with an access path to the center from which temperatures and soil-water contents were measured.

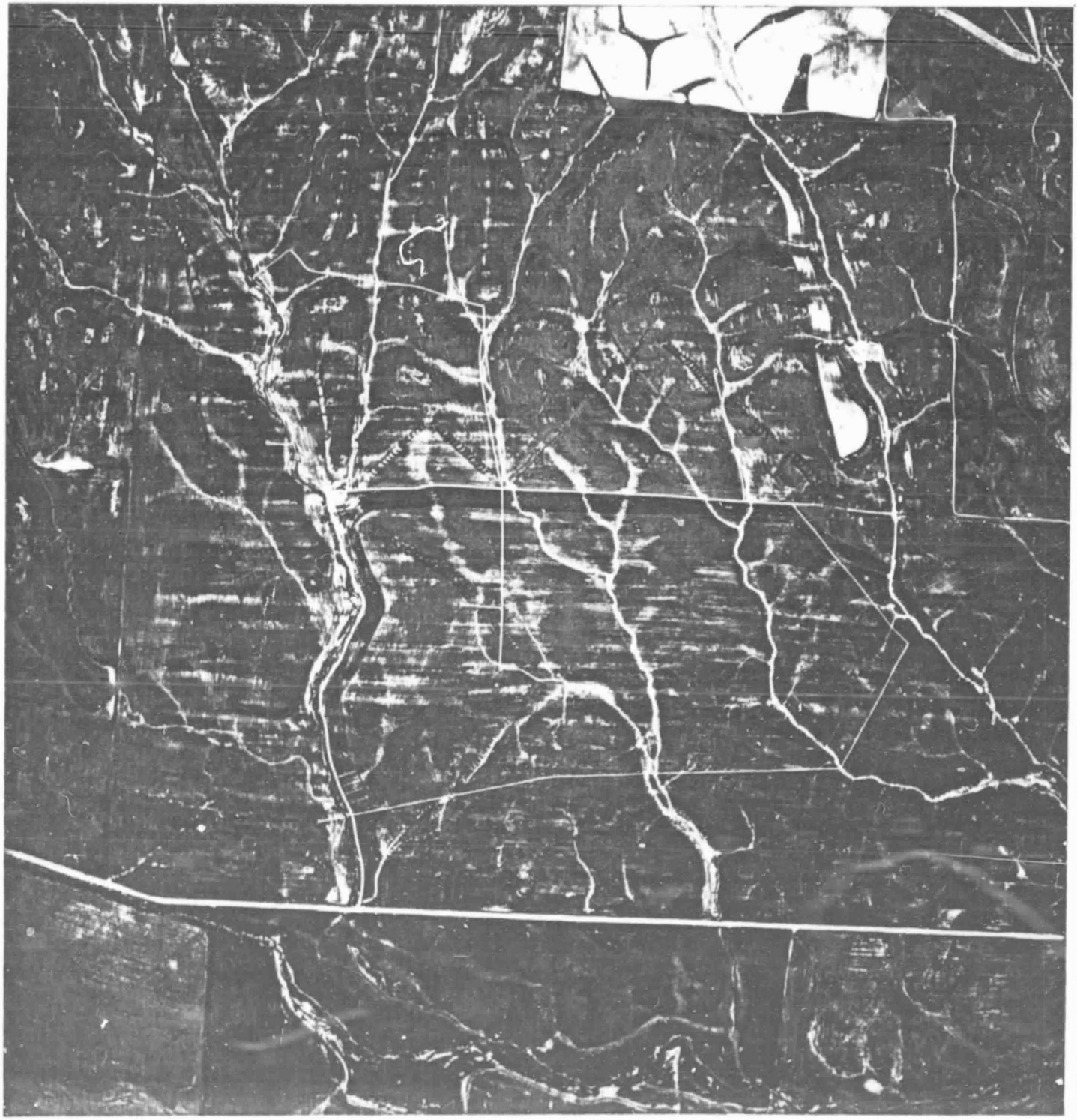

Figure 2. Aerial photo of the field taken on 10 March 1978. Variations in plant density are evident, as well as the headquarters area, roads, and paths.

Table 1. Identification symbol, slope, aspect, and direction of planting for the 16 ground measurement sites.

Site	Slope (%)	Aspect (Deg.)	General Planting Direction	
			Primary	Overplanting
R1	2	342	NE-SW	
R2	22	52	NW-SE	
R3	24	247	N-S	
R4	20	157	NW-SE	
T1	0	-	E-W	NW-SE
W1	4	232	E-W	NW-SE
B1	3	322	N-S	
E1	7	62	N-S	
S1	3	162	N-S	NW-SE
B2	2	160	NE-SW	
N1	6	347	NE-SW	
R5	36	47	NW-SE	
R6	24	7	N-S	
R7	0	-	E-W	
R8	0	-	E-W	
R9	1	132	N-S	

The soils are of the Sehorn-Balcom complex. They are well drained, gently to steeply sloping silty clay loams and clays on sandstone. The Balcom soil is classified as a fine-loamy, mixed, calcareous, thermic, typic Xerorthent, while the Sehorn is a fine, montmorillonitic, thermic, entic Chromoxerert. Soil samples taken prior to planting showed a variable but relatively low amount of nitrogen in the upper 25 cm of soil.

Facilities

Since the field was some distance from all services (power, etc.), the experiment had to be completely self-contained. Primary power was furnished by a 32 KW diesel generator. A portable building and two mobile trailers (which housed the electronic data logging and test equipment, oven, refrigerator, balance, battery chargers, and other miscellaneous devices) received power from the generator. To insure continuity in data collection, the data logger obtained power from storage batteries when the generator failed. The data logger could operate for 2-3 days without the generator. A 15 KW propane generator was available as a backup for the diesel generator. Diesel and propane were delivered by local fuel companies as needed. A radio telephone was installed for emergency purposes.

Measurements

Ground-based measurements were divided into two types: automatic and manual. Automatic refers to measuring several micrometeorological parameters near the trailers (R1) and at main site (T1, W1, B1, E1, S1, B2, and N1) and recording the 20-minute averages of these parameters

for the entire duration of the experiment. These parameters and the sites at which they were measured are given in Table 2.

The manual measurements are those which could not be recorded on a data logger, and were taken on a daily or less frequent basis. Table 3 describes the parameters measured, the locations, and the frequency of measurement. Table 4 gives information on the instruments used.

Crop and/or soil surface temperatures were measured with a portable infrared thermometer by going to the center of the plot and aiming the instrument at a spot about 3-5 m from the center in each of the four cardinal directions. Also, a down-looking (nadir) temperature was taken at four points at the plot center. In this way eight temperatures were obtained at each site, four at an angle and four at nadir.

Temperatures were measured every day from 17 October 1977 through 23 May 1978 except in inclement weather or if an equipment malfunction occurred. The data were taken about one hour prior to sunrise and again about one hour after solar noon. This amounted to 256 individual infrared thermometer readings daily. Additonally, dry bulb and wet bulb air temperature measurements were taken at each of the 16 sites during each of the twice-a-day measurement periods.

Soil water contents were measured with a neutron scattering probe and scaler, three times each week. Measurements were made in 20-cm increments to a maximum depth of 160 cm. In cases where the soil was shallow or a water table was present, the maximum measurement depth was less than 160 cm.

Table 2. Location of instruments used for automatic data logging of meterological parameters.

Parameter	Site							
	R1	T1	W1	B1	E1	S1	B2	N1
Incoming solar radiation	X	X					X	
Reflected solar radiation	X	X	X	X	X	X	X	X
Net radiation	X	X	X	X	X	X	X	X
Wind speed and direction	X	X					X	
Air temperature @ 150 cm	X	X	X	X	X	X	X	X
Soil temperature @ surface	X	X	X	X	X	X	X	X
Soil temperature @ 2 cm	X	X	X	X	X	X	X	X
Soil temperature @ 4 cm	X	X	X	X	X	X	X	X

Table 3. Frequency of manually obtained ground-based measurements.

Parameter	Sun	Mon	Tue	Wed	Thu	Fri	Sat
Surface temperature w/infrared radiometer, and dry and wet bulb temperatures with an aspirated psychrometer presunrise and @ 1230-1300 hr	X	X	X	X	X	X	X
Soil moisture w/neutron meter every 20-cm depth to 160 cm		X		X		X	
Ten plant samples from each site for height, dry weight, green leaf area, and growth stage		X			X		
Soil temperature w/thermistor probe @ 2- and 4-cm depth at sites R2 through R9	X	X	X	X	X	X	X
Albedo at sites R2 through R9 w/portable unit on clear days							
Insect sweeps and pathogen identification			X				
From weather station @ R1 site; maximum-minimum temperatures and evaporation pan (also, weekly record from hygrothermograph).	X	X	X	X	X	X	X
Raingages at all 16 sites (as appropriate)							
NASA aircraft at 1.4 km to measure surface temperature @ presunrise and @ 1300 hours			X			X	

Table 4. Manufacturer and model of ground-based instruments used.

Parameter	Instrument	Manufacturer	Model
Automatic Measurements			
Incoming solar radiation	Pyranometer	Eppley	8-48
" " "	"	Lambda Inst. Co.	7407
" " "	"	Spectran	4048
Reflected solar radiation	"	Eppley	8-48
" " "	"	Spectran	4048
Net radiation	Miniature Net Radiometer	Micromet Inst.	--
Wind speed & direction	Propeller Vane	Gill	35003
Air & soil temperature	Copper-constantan thermocouples	Thermo Electric	
Manual Measurements			
Surface temperature	Infrared thermometer	Telatemp	44 and AG-42
Dry and wet bulb temp.	Aspirated psychrometer	Bendix	566
Soil water content	Neutron Moisture Meter	Troxler	2601/1255
Soil temperature	Thermistor probe	Extech	1200-1108
Albedo	Pyranometer	Spectran	8-48
Maximum-minimum air temp.	Mercury Thermometers		--
Air temp. & humidity	Hygrothermograph	Belfort	--
Rainfall	Raingauge	Tru-Chek	--
Evaporation	Class A pan	--	--

Ten plant samples, randomly selected from each of the 16 sites, were gathered twice weekly and transported to Davis for analysis. Information gathered from these samples was phenological growth stage, plant height, dry weight, green leaf area, number of green leaves per plant, number of tillers, and number of heads. Shortly after emergence a plant density count was made at each site. At three locations at the main site (T1, W1, and S1) there were parts of the target area that were overplanted (the planter went over it twice).

At the end of the measurement period, a portion of each site was hand harvested. Five consecutive "squares" were taken in each of the four cardinal directions, starting one meter from where we normally stood to take plant temperatures. All plants were removed from these 20, one meter squares at each location, the number of heads in each square meter counted, and the samples labeled and bagged for further processing.

Following harvest, all samples were threshed, the number of seeds counted, and their weight and water content determined. From these data, the following information was obtained: Seed water content; number of heads per square meter; number of seeds per head; number of seeds per square meter; bushel weight; and yield. The last two items were corrected to a gravimetric seed water content of 0.125 to allow comparisons between sites.

Albedo, the ratio of reflected to incoming solar radiation, was measured with a pyranometer attached to a pole with the sensor facing the crop. The device was hand-held over the crop and measurements were made at six locations around the footpath leading to the center of the remote

plots. Incoming solar radiation was measured twice at each plot. The measurements were made near solar noon on clear days.

In order to assess crop damage due to insects, sweep net samples were taken once a week and insects were counted and identified. The top 20-30 cm of the plants were sampled using 25 sweeps with the net. Approximately 12.5 m^2 were sampled at each site, once each week. Pathogen activity was noted and identification was made by the county agricultural agent.

A routine weather station was maintained northeast of the headquarters trailer. Daily observations of maximum and minimum air temperatures and pan evaporation were recorded. Also, weekly records from a hygrothermograph were collected.

Raingages at each of the 16 sites were read after each rain.

Field cultural operations

The field had been disc-plowed during the summer 1977. The farmers, anticipating another year of drought, planted Briggs barley (Hordeum vulgare L.) instead of wheat (the drought tolerance of barley is greater than wheat), during the week of 1-7 December 1977 at the rate of 112 kg/ha. They also incorporated 35.6 kg/ha of nitrogen and 39.4 kg/ha of phosphorous fertilizer in the form of ammonium phosphate. On 1 February 1978, 44.8 kg/ha additional nitrogen was applied by aircraft, because much of the original fertilizer had been leached from the root zone by heavy rains. During the following 2 weeks, the barley turned dark green. Areas missed in the 1 February application were aerially fertilized with 112 kg/ha nitrogen in the form of ammonium nitrate on 18 February. On

20 February 1978, a herbicide was aerially sprayed to control broadleaf weeds. From 23 to 30 May 1978, the barley was harvested.

Weather

The weather during the growing season was characterized by above normal rainfall and temperature. A summary of the rainfall is given in Table 5 for each site by months. During October and November 1977 there were only two raingages installed, so the numbers in parentheses are estimated based on the relationships between gages for later months. It turned out that this year indeed marked the end of the drought that California had experienced for several years. In fact, our experimental site received nearly 70% more rain (675 mm) than normal (400 mm) during the 7-month period of measurement.

The overabundance of rain, the second wettest year on record, caused several problems. First, crop water-stress conditions did not develop at any of the sites. Second, the large number of inclement days resulted in fewer aircraft overflights than were planned. Third, the excess water caused severe flooding and erosion problems. Five of the sites, R1, B1, B2, R7, and R9 developed water tables that were observable in the neutron access tubes. Erosion in the gullies caused two sites, B2 and R7, to be relocated, creating some discontinuity in the data. All sites with high water tables had poor stands of barley, and a severe weed problem.

Low Altitude Imagery

Low altitude thermal imagery of the site was acquired from a Cessna 402 aircraft. Data were taken throughout the growing season, from planting to harvest, except during April when the aircraft was grounded

Table 5. Summary of rainfall at the sites for the period October 1977 through April 1978.

(mm)

	Oct 77	Nov 77	Dec 77	Jan 78	Feb 78	Mar 78	Apr 78
Gate	4.6	76.5	70.6	229.4	111.5	84.3	54.1
HQ	(5.6)	(86.9)	77.5	262.9	116.6	84.9	54.1
R1	5.6	80.3	67.8	230.6	113.5	84.1	55.6
R2	(5.6)	(85.6)	74.2	254.0	122.2	88.6	56.9
R3	(5.8)	(88.4)	74.2	267.2	123.4	93.2	58.7
R4	(4.6)	(68.6)	57.1	210.1	93.7	77.5	53.8
T1	(5.6)	(87.4)	75.9	262.1	120.9	83.1	58.9
W1	(5.3)	(82.0)	70.1	247.1	113.5	82.8	57.1
B1	(5.3)	(82.3)	72.4	245.9	114.3	84.1	57.4
E1	(5.3)	(83.8)	69.6	248.9	121.9	83.8	56.4
S1	(5.3)	(82.0)	73.4	242.1	115.6	83.6	56.6
B2	(5.6)	(85.3)	71.6	255.0	121.9	85.6	56.4
N1	(5.1)	(78.7)	67.6	234.2	112.5	83.6	58.9
R5	(6.1)	(92.2)	82.6	272.3	129.3	93.5	59.7
R6	(6.6)	(100.3)	82.8	301.5	142.2	94.5 93.2	63.0
R7	(5.3)	(82.6)	69.9	246.6	116.8	87.1	58.7
R8	(5.6)	(87.6)	74.7	264.2	120.9	86.1	56.6
R9	(5.3)	(81.8)	71.9	241.3	116.3	86.3	54.4
$\bar{x}$	5.6	84.1	72.4	251.0	118.1	86.4	57.2
$\Sigma\bar{x}$	5.6	89.7	162.1	413.0	531.1	617.5	674.6

for maintainance. More than 60 flights were completed, of which 55 provided usable data. Flights were made both prior to sunup and about one hour after solar noon. Thermal imagery was acquired with a Texas Instruments Model RS-25 infrared scanner operating in the 10.5-12.5 μm bandpass region. The instrument had an instantaneous field of view (IFOV) of about 2 x 2 m at a flight altitude of about 1.2 km (4000 ft.) and a temperature accuracy of about 0.2°C. The scanner contained two blackbody calibration sources with platinum resistance thermometers for continuous inflight calibration. At the completion of each flight, atmospheric temperature and humidity were measured at various levels down to near ground level. These were used to correct the thermal-IR data for absorption by atmospheric water vapor.

The RS-25 scanner data were recorded on magnetic tape in analog form, converted to digital form, and processed by using digital image techniques. The first step in converting the analog data to a computer-compatible digital format was to average it using "sample and hold" techniques, which integrate the analog signal for a predetermined period of time. The integrated signal was then measured by an A/D converter which assigned a value to represent the signal's relative amplitude. The "sampling" period represents one picture element (or pixel), and the pixel amplitude is converted to a digital value ranging from 0 to 255 (8 bits). The thermal infrared data was processed on an HP-3000 computer system equipped with a COMTAL video display, two 1600 BPI tape drives, and two 50 megabyte disk memories. The software program, called IDIMS,

acted upon the digital image. Since the RS-25 scanner collected data in a scan-line-to-line sequence, each line represented a row in the digital image. Similarly, the selected sample interval for digitizing determined the number of pixels in each scan line. Since each scan line contained the same number of picture elements, the pixels made up the columns in the image array.

Seven separate processing steps were used to generate the final output images reported here. They were:

(1) Scene selection. All recorded digital image data were reviewed on the COMTAL display. Thermal calibration, high frequency image jitter, bad or missing scan lines, image noise, and general image appearance were used as selection factors.

(2) Scene reduction. The portion of the scene outside the area of interest was edited out. This conserved processing time.

(3) Sweep distortion correction. Geometrical distortions caused by the constant angular velocity of the scanner mirror were corrected.

(4) Transfer of black body digital values to the reduced scene. This step was required since the position of the calibration signals on the original total scene caused them to be edited out in Step 2, above.

(5) Thermal calibration. The basic digitized image was created with 256 (8 bit) grey levels. These levels were proportional to the energy received by the RS-25 scanner from each point on the ground. The thermal black body references were also imaged within 256 grey levels, but their temperatures were known. Thus, all image grey levels could be transformed into apparent temperatures by using the black bodies as

function generators. The output image, then, had real-valued pixels which represented the apparent temperatures on the ground as seen by the RS-25 scanner.

(6) Atmospheric correction. The foregoing apparent temperatures were corrected for atmospheric effects by use of the LOWTRAN 4 computer code. Multi-level, aircraft acquired, values of atmospheric temperature and humidity were utilized. The effects of CO_2, O_3 and aerosols were accounted for in the code.

(7) Presentation of the processed image. Final results were presented in the following forms:

a) Pseudo-colored video display, where each color represents a discrete temperature interval.

b) Total scene display or selected areas expanded to fill video screen size.

c) Line printer output of apparent temperature values or temperature differences.

d) Single pixel values selected by the operator.

High Altitude Imagery

High altitude thermal imagery of the site was acquired with the HCMR prototype scanner flown on NASA's U-2 aircraft at an altitude of 20 km (pixel size 70 x 70 m). Data were acquired the afternoon of 16 May 1978, simultaneous with the HCMM spacecraft pass. The data tapes from these flights were made computer-compatible by NASA/GSFC, and returned to NASA/Ames where they were processed in a manner similar to that described

in the previous section. Air temperature, and dew point were acquired from the Oakland, California National Weather Service soundings for use in computing atmospheric corrections to the thermal data by the LOWTRAN 4 computer code.

Spacecraft Imagery

Multi-staged experiments were conducted on the days and from the platform given in Table 6.

Table 6. Dates and platforms for acquiring multi level aircraft and spacecraft data over the experimental field.

Date	Ground	Cessna	U-2	HCMM
5/16/77 Postnoon	X	X	X	X
5/20/77 Presunrise	X	X		X
5/20/77 Postnoon	X	X		X

The spacecraft data were handled in a manner similar to the aircraft data except that NASA/GSFC provided computer-compatible tapes. The mapping of the grey levels to corresponding temperatures was done using a set of parameters and an equation supplied by Goddard:

$$T(I) = K_2/\{\ln[K1/(1-K_3)+1]\} \qquad (1)$$

where T is the Kelvin temperature, 1 the pixel byte level, K_1 = 14421.587, K_2 = 1251.1591, and K_3 = -118.21378.

RESULTS AND DISCUSSION

Soil Moisture Estimation

The objective of monitoring soil moisture in the surface layer of bare soil on a repetitive basis was addressed in the Fall of 1977 prior to emergence of the barley. Soil samples were taken from the surface to 4-cm at about 1100 (Jackson et al., 1976) for 16 days over a 30-day period. Soil moisture was determined on a weight basis and expressed as gravimetric water content. Two temperature parameters were used: the surface minus air temperature in the afternoon $(T_S - T_A)_{pm}$ (Idso et al., 1975; Reginato et al., 1976), and the afternoon-morning surface temperature difference as normalized by the method of Idso et al., 1976. The results are shown in Figure 3. In theory, both temperature parameters should decrease with increasing water content. With some imagination, one can see a decrease with increasing water content for the afternoon surface-air temperature difference, but not for the day-night differences. The scatter is the result of the adverse weather conditions. Of the 16 days of measurement, only two were relatively clear. These two days are indicated by the solid circles in Figure 3. Considering only the two clear days, the temperature parameters did decrease with increasing water content. The two points compare well with published data (Idso et al., 1976).

The scatter of the data in Figure 3 emphasizes the fact that thermal infrared techniques for estimating soil water content yield reliable results only under clear sky conditions. Thermal infrared data from

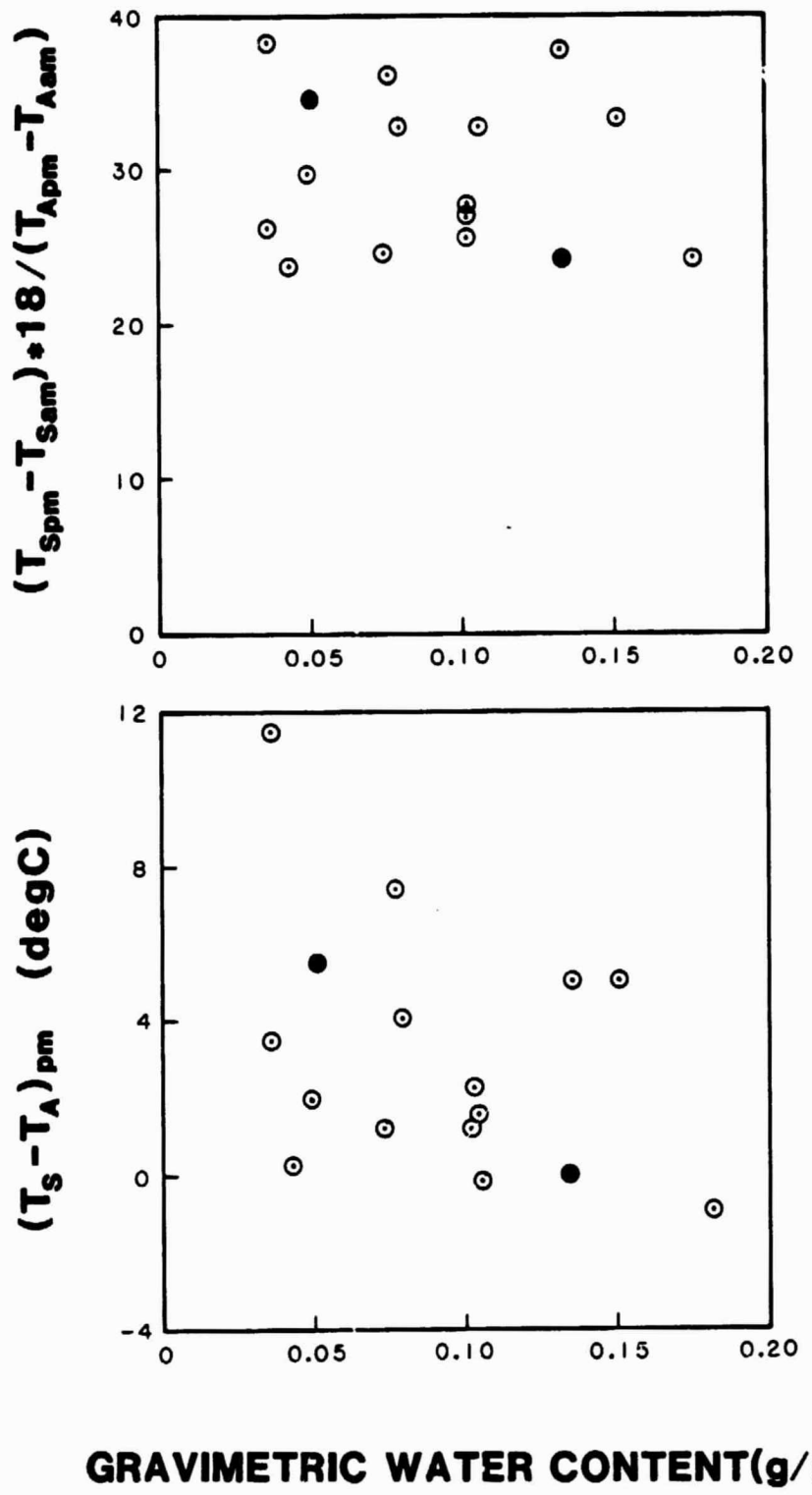

Figure 3. The p.m. minus a.m. surface temperature difference normalized with the air temperature difference (top) and the surface minus air temperature difference (bottom) as a function of gravimetric water content. The solid symbols represent clear day data.

satellites can only be obtained under clear skies. Thus, this technique is most useful in areas with few clouds. Such areas normally are arid and, therefore, soil moisture information is of particular importance.

Plant Water Stress

Data relating to our objective of monitoring plant water stress were collected from January through May of 1978. In the course of our investigations it became evident that the stress-degree-day concept as proposed by Idso et al., 1977 and Jackson et al., 1977 was an insufficient indicator of stress, especially under humid conditions. Consequently we derived a crop water stress index (CWSI) from energy balance considerations (Jackson et al., 1981, in press) and empirically from a large data set (Idso et al., 1981, in press). A summary of the development of this index will be presented here not only for the purpose of quantifying plant water stress but also to provide a basis for interpreting spacecraft thermal data obtained over different climate regions.

The energy balance for a crop canopy can be written

$$R_n = G + H + \lambda E \tag{2}$$

where R_n is the net radiation (W m^{-2}), G is the heat flux below the canopy (W m^{-2}), H is the sensible heat flux (W m^{-2}) from the canopy to the air, λE is the latent heat flux to the air (W m^{-2}), with λ being the heat of vaporization. In their simplest forms, H and E can be expressed as

$$H = \rho c_p (T_C - T_A)/r_a \tag{3}$$

and

$$\lambda E = \rho c_p (e_c^* - e_A)/[\gamma(r_a + r_c)] \tag{4}$$

where ρ is the density of air (kg m^{-3}), c_p the heat capacity of air (J $kg^{-1}C^{-1}$), T_c the surface temperature (°C), T_A the air temperature (°C), e_c^* is the saturated vapor pressure (Pa) at T_c, e_A the vapor pressure of the air (Pa), γ is the psychrometric constant (PaC^{-1}), r_a is the aerodynamic resistance (s m^{-1}), and r_c is the canopy resistance (s m^{-1}) to vapor transport. A detailed discussion of procedures leading to equations (2), (3), and (4) is given by Monteith (1973).

Combining (2), (3), and (4), assuming that G is negligible, and defining Δ as the slope of the saturated vapor pressure - temperature relation $(e_c^* - e_A^*)/(T_c - T_A)$, units of PaC^{-1}, we obtain

$$T_c - T_A = \frac{r_a R_n}{\rho c_p} \cdot \frac{\gamma(1 + r_c/r_a)}{\Delta + \gamma(1 + r_c/r_a)} - \frac{e_A^* - e_A}{\Delta + \gamma(1 + r_c/r_a)} \qquad (5)$$

which relates the difference between the canopy and the air temperatures to the vapor pressure deficit of the air $(e_A^* - e_A)$, the net radiation, and the aerodynamic and crop resistances.

The upper limit of $T_c - T_A$ can be found from (5) by allowing the crop resistance r_c to increase without bound, i.e., as $r_c \to \infty$

$$T_c - T_A = \frac{r_a R_n}{\rho c_p} \qquad (6)$$

The lower bound, found by setting $r_c = 0$ in (5) (the case of wet plants acting as a free water surface), is

$$T_c - T_A = \frac{r_a R_n}{\rho c_p} \cdot \frac{\gamma}{\Delta + \gamma} - \frac{(e_A^* - e_A)}{\Delta + \gamma} \qquad (7)$$

Equations (5) and (7) describe a linear relation between $T_c - T_A$ and the vapor pressure deficit, $e_A^* - e_A$. Thus, for a particular temperature, the lower bound is a line extending from the intercept at $e_A^* - e_A = 0$ (saturated air) to a value of $e_A^* - e_A = e_A^*$ (completely dry air). Since Δ appears in both the slope and the intercept, both terms are temperature dependent.

Equation (7) represents the case of evaporation from a free water surface, which is not necessarily the case for potential evaporation from a crop. In irrigated areas, the soil may be adequately supplied with water, with the plant surfaces being dry. In this case the canopy resistance is probably not zero (van Bavel and Ehrler, 1968), but has a value that we will call the canopy resistance at potential evapotranspiration (r_{cp}). The value of r_{cp} will probably be different for different crops, and may change with crop variety. Setting $r_c = r_{cp}$ in (5) we have

$$T_c - T_A = \frac{r_a R_n}{\rho c_p} \cdot \frac{\gamma^*}{\Delta + \gamma^*} - \frac{e_A^* - e_A}{\Delta + \gamma^*} \qquad (8)$$

where

$$\gamma^* = \gamma(1 + r_{cp}/r_a) \qquad (9)$$

A crop with adequate water will transpire at the potential rate for that crop. As water becomes limiting, the actual evapotranspiration

will fall below the potential rate. A measure of the ratio of actual to potential evapotranspiration should, therefore, be an index of crop water status. Combining (2), (3), and (4) and solving for λE yields

$$\lambda E = \frac{\Delta R_n + \rho c_p (e_A^* - e_A)/r_a}{\Delta + \gamma (1 + r_c/r_a)} \qquad (10)$$

which is the Penman-Monteith equation for evapotranspiration in terms of canopy and aerodynamic resistances (Monteith, 1973: Thom and Oliver, 1977). Taking the ratio of actual (λE for any r_c) to potential (λE_p for $r_c = r_{cp}$) gives

$$E/E_p = \frac{\Delta + \gamma^*}{\Delta + \gamma(1 + r_c/r_a)} \qquad (10)$$

with γ^* defined by (9). Jensen (1974) and Howell et al (1979) discussed (11) for the case of $r_{cp} = 0$, i.e., $\gamma^* = \gamma$. Rearranging (11) will give r_c in terms of E/E_p, a result reported by van Bavel (1967), Szeicz and Long (1969), and Russell (1979), again with $r_{cp} = 0$. Van Bavel measured E with lysimeters and calculated the canopy resistance.

The ratio E/E_p ranges from 1 (ample water, $r_c = r_{cp}$) to 0 (no available water, $r_c \to \infty$). In studying plant-water relations one thinks of a plant as going from a no-stress to a stressed condition. Therefore, it is esthetically pleasing for a stress index to go from 0 to 1. We consequently define a crop water stress index (CWSI) as

$$CWSI = 1 - E/E_p = \frac{\gamma(1+ r_c/r_a) - \gamma^*}{\Delta + \gamma(1 + r_c/r_a)} \qquad (12)$$

To calculate the CWSI or E/E_p using (11) or (12) requires a value for the ratio r_c/r_a. This is obtained by rearranging (5) with the result

$$\frac{r_c}{r_a} = \frac{\gamma\, r_a R_n/(\rho c_p) - (T_c - T_A)(\Delta + \gamma) - (e_A^* - e_A)}{\gamma\,[(T_c - T_A) - r_a R_n/(\rho c_p)]} \qquad (13)$$

giving the ratio r_c/r_a in terms of net radiation, canopy and air temperatures, vapor pressure deficit, and the aerodynamic resistance. In practice, r_c/r_a is evaluated using (13) and substituted into (12) to obtain the CWSI.

The slope of the saturated vapor pressure - temperature relation (Δ) appears in most of the equations in the previous section. As a first approximation, Δ can be evaluated at the air temperature (T_A). When the temperature difference ($T_c - T_A$) is large (for the case of well-watered crops at high vapor pressure deficits) a better approximation is to evaluate Δ at $(T_c + T_A)/2$. Obviously, when T_c is near T_A the two approaches yield similar results. Taking the average of the canopy and air temperatures is sufficient for (5), (7), (8), and (13), but (11) and (12) pose a problem. Following closely the development of (11) from (10), we find that Δ in the numerator should be evaluated at the average of the air temperature and the canopy temperature that would obtain if the crop was evaporating at potential. The Δ in the denominator should be evaluated at the average of the actual measured canopy temperature and the air temperature. Keeping Δ as the value at the measured temperatures and Δ^* as the value using the calculated canopy temperature at

potential, the numerator of (11) becomes $\Delta^* + \gamma^*$ and the numerator of (12) becomes $\gamma(1 + r_c/r_a) - \gamma^* + (\Delta - \Delta^*)$.

The evaluation of Δ^* is complicated by the fact that T_c at potential may not be known. This can be calculated using an iterative procedure with (8) by evaluating Δ at T_A, calculating T_c, evaluating a new Δ at $(T_c + T_A)/2$, and recalculating T_c until an acceptable value is obtained. In practice the use of (11) and (12) with Δ evaluated at the average of the measured canopy temperature and the air temperature will yield similar results for both the low and high values of the indices, with the maximum error occurring near 0.5. At the midpoint, the difference between the two methods of calculation will be within 0.06, e.g., 0.48 for the one value of Δ and 0.54 when Δ and Δ^* are used. The results reported here are in terms of Δ evaluated at both the canopy temperature at potential and at the average temperature of the measured canopy and air temperatures.

A graphic example of the CWSI is given in Figure 4. The four lines emanating from the ordinate and ending at about 4.24 kPa were calculated using (5) with $R_n = 600\ Wm^{-2}$, $r_a = 10 sm^{-1}$ and r_c taking on the values shown at the end of the lines (i.e., 5, 50, 500, ∞ canopy resistances). The lower line ($r_c = 5$) represents a well-watered crop transpiring at the potential rate. The topmost line ($r_c = \infty$) represents the case of a nontranspiring crop. If a canopy temperature is measured at a vapor pressure deficit of 3 and found to be 3°C below the air temperature, the datum would plot at B. If the plants were not stressed the point would

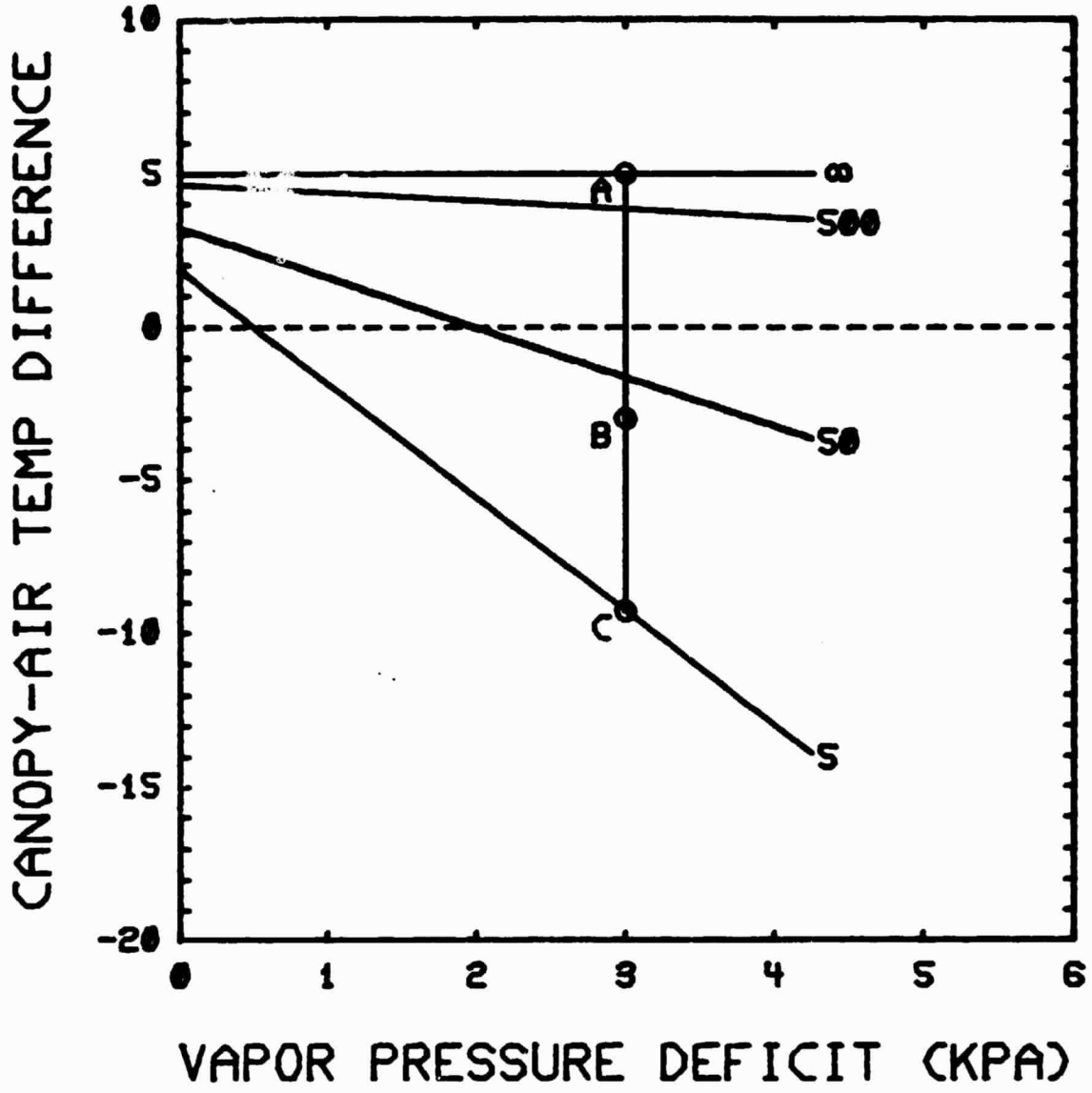

Figure 4. Theoretical relationship between the canopy-air temperature difference and the vapor pressure deficit. Numbers at the end of each line indicate the value of the canopy resistance (r_c) used for the calculations. Point B represents a data point for which a value of the crop water stress index (CWSI) can be obtained by ratioing the distance BC to AC. See text for mathematical derivation of the CWSI. All calculations were for air temperature (T_A) of 30°C, net radiation (R_n) of 600 Wm^{-2}, and an aerodynamic resistance (r_a) of 10 sm^{-1}.

be at C, and if no transpiration could take place, the point would be at A. The CWSI is BC/AC.

The CWSI was calculated for all sites having valid net radiation data, beginning about 15 February. Data for clear days on plot T1 are shown in Figure 5. Except for two data points (days 100 and 112) the results show a slight increase in the CWSI until about day 140. At this time the plants had begun to senesce. As senescence progressed and the plants matured the CWSI increased. Data for other plots were similar to those shown in Figure 5. The value of the CWSI depends on the choice of the canopy resistance at potential evaportranspiration (r_{cp}). We used a value derived from irrigated wheat data (5 sm^{-1}), since a value has not been established for barley. A larger value of r_{cp} would have resulted in smaller values of the CWSI. Since more than adequate moisture was available most of the season, and since all plots for which the CWSI was calculated had similar values of the CWSI, it appears that our choice of r_{cp} was low.

Equation (5) and Figure 4 provide an aid for interpreting thermal infrared data over different climatic regions. In humid regions, the vapor pressure deficit is low and plant temperatures are generally warmer than air temperatures. The range of canopy-air temperature differences are small and therefore thermal discrimination of different vegetation types or stages is difficult, if not impossible. In an arid area, where the vapor pressure deficit is usually high, discrimination between well watered and stressed vegetation is possible. Also

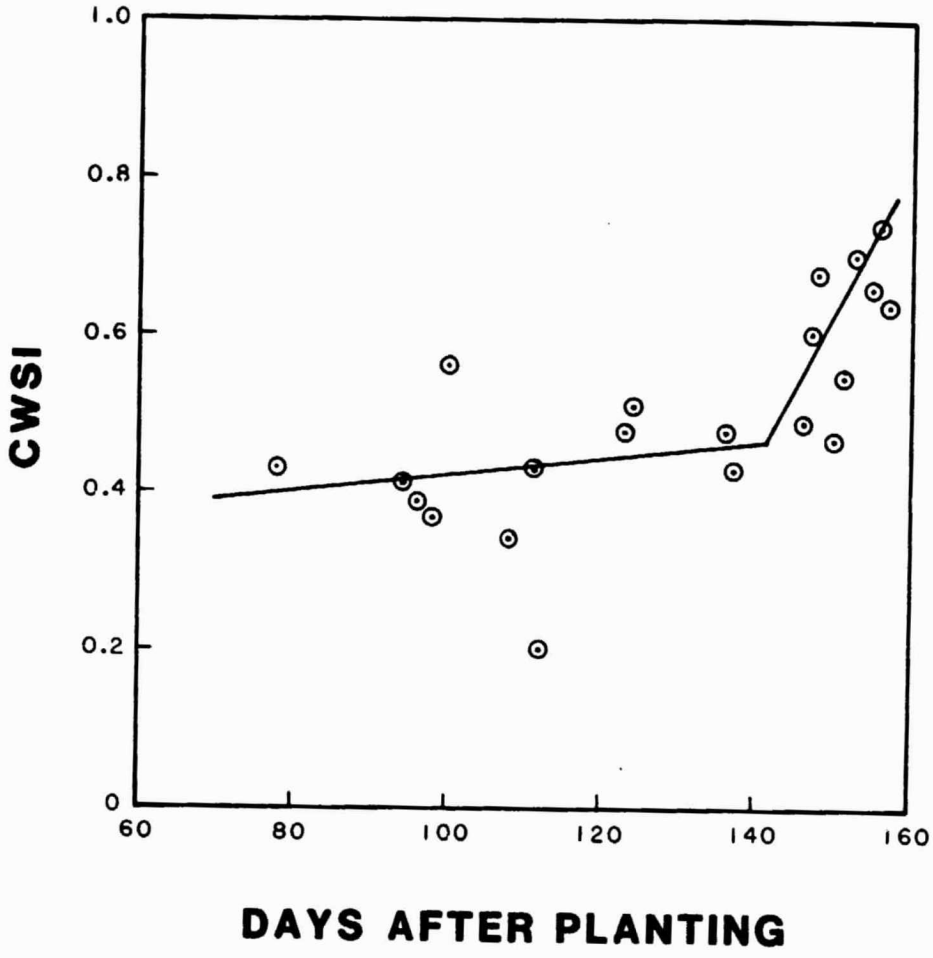

Figure 5. The crop water stress index (CWSI) as a function of days after planting for site T1. The lines were drawn by eye with the slope change occurring when senescence began.

senescing vegetation could be discriminated from actively growing vegetation.

Plant Growth and Yield

Plant samples were taken twice each week over the growing season. All plant measurements were made by personnel at the University of California, Davis. Details of these measurements are given in an excellent thesis written by Carol Whitman (Whitman, 1981) and submitted toward fulfillment of requirements for a Master of Science degree. Pertinent data abstracted here are the critical plant growth stages (Table 7), the final yield of grain and total dry matter (Table 8), and a composite of sites according to drainage and irradiance (Table 9). The growth stage data presented in Table 7 show that the time required to reach heading and anthesis was different for the different sites; also yields were different for the various sites. For the most part, differences were due to slope and aspect of the terrain, and the fact that several sites had high water tables during much of the season. Temperature measurements did not distinguish these differences.

The crop water stress index, because of the recentness of its development, has not been incorporated into yield models. The predecessor of the CWSI, the stress-degree-day (SDD), has been used in yield models. Although some shortcomings of the SDD were discussed earlier in this report, we used the model and data of Idso et al. (1980) to show that the yields obtained in this experiment fall well within the range of yields obtained for a number of crops (figure 6). The encircled open diamonds

Table 7. Critical development stages, in days after planting, for barley grown at Dunnigan, 1977-78. Day 0 was 7 December 1977.

Site	Planting	Begin Tillering	Rapid Tillering	Jointing	Boot	Heading	Anthesis	Maturity
R1	0	32	54	98	123	139	146	158
R2	0	32	51	81	108	126	134	151
R3	0	32	51	78	104	123	132	151
R4	0	32	51	74	100	119	127	148
R5	0	32	51	80	106	125	134	153
R6	0	32	51	80	106	125	134	150
R7	0	32	51	83	108	127	135	158
R8	0	32	51	82	108	126	134	150
R9	0	32	51	85	113	135	144	154
T1	0	32	51	78	104	123	131	155
W1	0	32	51	78	104	123	131	149
B1	0	32	51	86	114	133	142	152
E1	0	32	51	84	111	129	137	158
S1	0	32	51	80	105	124	132	156
B2	0	32	51	80	105	124	132	160
N1	0	32	51	86	114	130	138	159

Table 8. Final yield and total dry matter for barley grown at Dunnigan, California, 1977-78.

Site	Yield (gm^{-2})	Total Dry Matter (gm^{-2})
R1	104.5	364
R2	321.5	1057
R3	372.7	1621
R4	417.5	1373
R5	315.3	1049
R6	234.0	883
R7	232.5	599
R8	367.2	1249
R9	118.8	634
T1	325.1	1111
W1	317.2	988
B1	116.2	433
E1	279.1	546
S1	348.5	782
B2	—	570
N1	243.5	706

Table 9. The effects of irradiance and drainage conditions on growth parameters of barley grown at Dunnigan, 1977-78. Means followed by the same lower case letter are not significantly different.

Drainage	Irradiance	Site	Height (cm)	Max tillers/ plant	% survival of tillers	Max no. of green leaves/plant	LAI	Mean area/ leaf (cm^2)	Dry matter production ($g\ m^{-2}$)
Good	High	R3,R4	114 a	4.5 a	7.2 a	14.0 a	2.4 a	19.2 a	649 a
Good	Medium	R8,T1,W1,E1,S1	106 a	3.4 b	4.5 ab	10.6 b	1.8 b	14.0 b	428 b
Good	Low	R2,R5,R6	108 a	3.3 ab	2.8 b	11.3 ab	1.5 b	13.3 b	401 b
Poor	Medium	R1,R7,R9,B1,B2,N1	82 b	3.0 b	0 c	8.3 c	0.9 bc	9.3 c	210 c

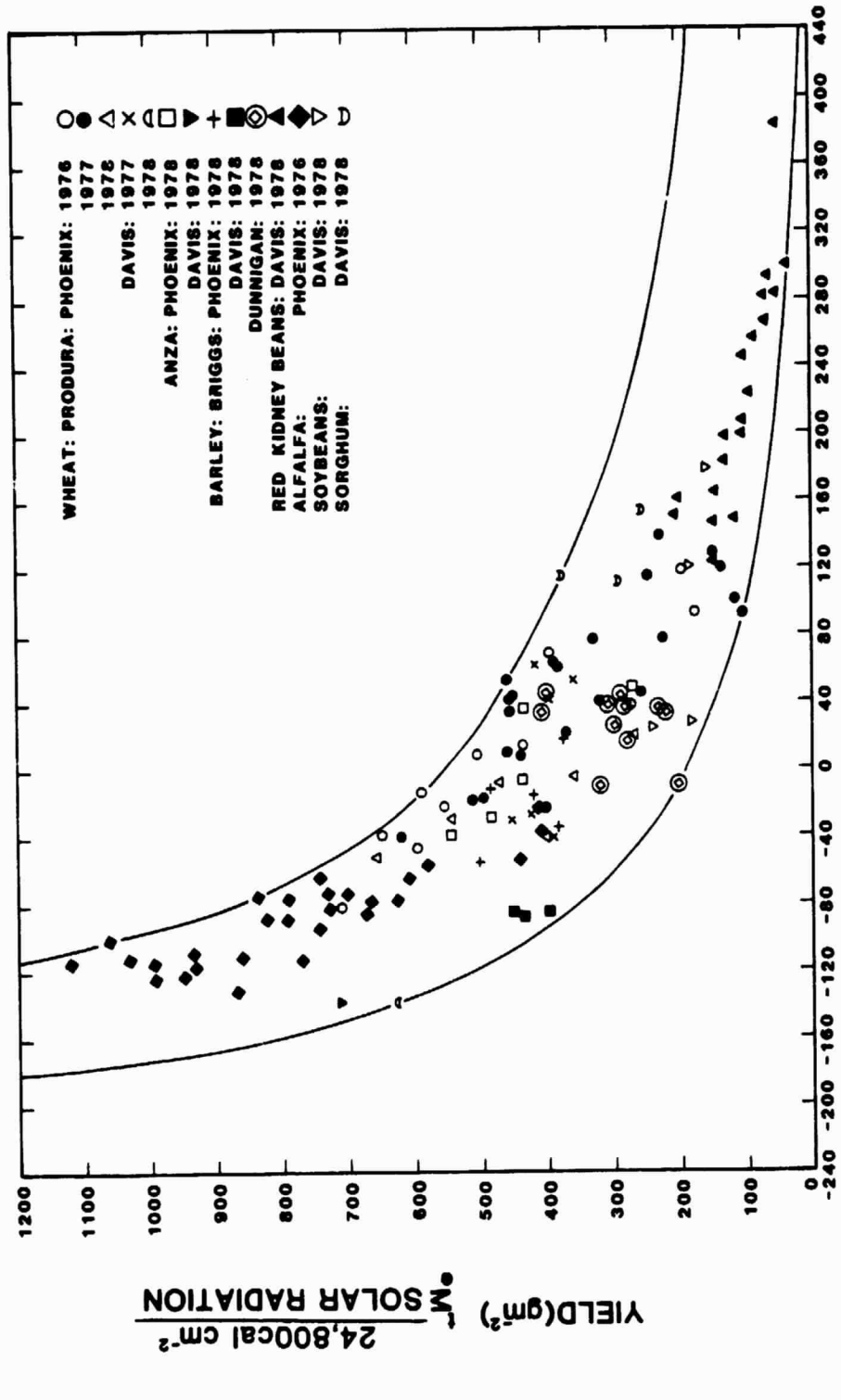

Figure 6. Crop yield as normalized for the total receipt of solar radiation during the vegetative period of growth versus the summation of stress-degree-days accumulated during the reproductive period of growth.

indicate data for 11 of the 16 sites. Of the five sites not shown, one was not hand-harvested before the farmer operated combine arrived. Four other sites were in low poorly drained areas. These sites had a poor stand of barley but a lush stand of weeds. The foliage (in contrast to crop) temperatures were low, consequently the SDD's were low. The SDD yield model would predict high yields under these weedy conditions, whereas the actual barley yields were low. These results demonstrate that weed growth can be a serious confusing factor when canopy-temperature-based yield models are used.

Although the yields from 11 sites fall within the range shown in figure 6, yield differences between the sites were not differentiated by the accumulated stress degree days. As implied earlier, the differences probably were due to the effects of terrain slope and aspect. To examine this possibility data from the sites were segregated into four groups that represented good and poor drainage, and high, medium, and low levels of irradiance. These data are given in table 9. The slope and aspect for each site are given in table 1. Grouping the data as in table 9 shows that barley growth on south-facing slopes was generally better than on north-facing slopes, and that poorly drained soils can adversely affect plant growth. These data point out the complexities of the effect of slope and aspect on yield models that use remotely sensed data as inputs. Quantifying the effect of slope and aspect would not be feasible using only 1 year of data. Had the experiment been conducted the previous year under conditions of drought, the south-facing slopes would probably have

been stressed and thus produce low yields, whereas the poorly drained sites may have been the only ones with adequate water, and thus would have had the highest yields.

Comparison of Ground and Aircraft Acquired Surface Temperatures

Ground-based temperature measurements offer the opportunity to measure vegetation temperatures with a minimum of soil background influence. This is accomplished by viewing a target at an angle, after the plants have attained sufficient height. The crop water stress index, and other temperature-based plant indices, depend on a measure of the temperature of only foliage. Scanners aboard aircraft and satellites are essentially nadir-looking, and soil background may be observable. This problem was studied by Millard, Hatfield, and Goettleman (1979), and Millard et al., (1980). The latter compared ground-measured canopy temperatures with those obtained from an airborne scanner and concluded that, when 85% or more of the soil surface is covered by vegetation, airborne and ground measurements differed by less than 2°C. Further analysis indicated that ground-based nadir measurements were nearly the same as the airborne data.

When the soil surface is moist, its temperature will be closer to the vegetation temperature than when it is dry. The frequent rain at the experimental site kept the soil surface moist much of the time. Toward the latter part of the season, plant senescence and higher sun elevations (more radiation striking the soil) caused the nadir-looking temperatures to exceed those measured at an angle (Figure 7). The effect

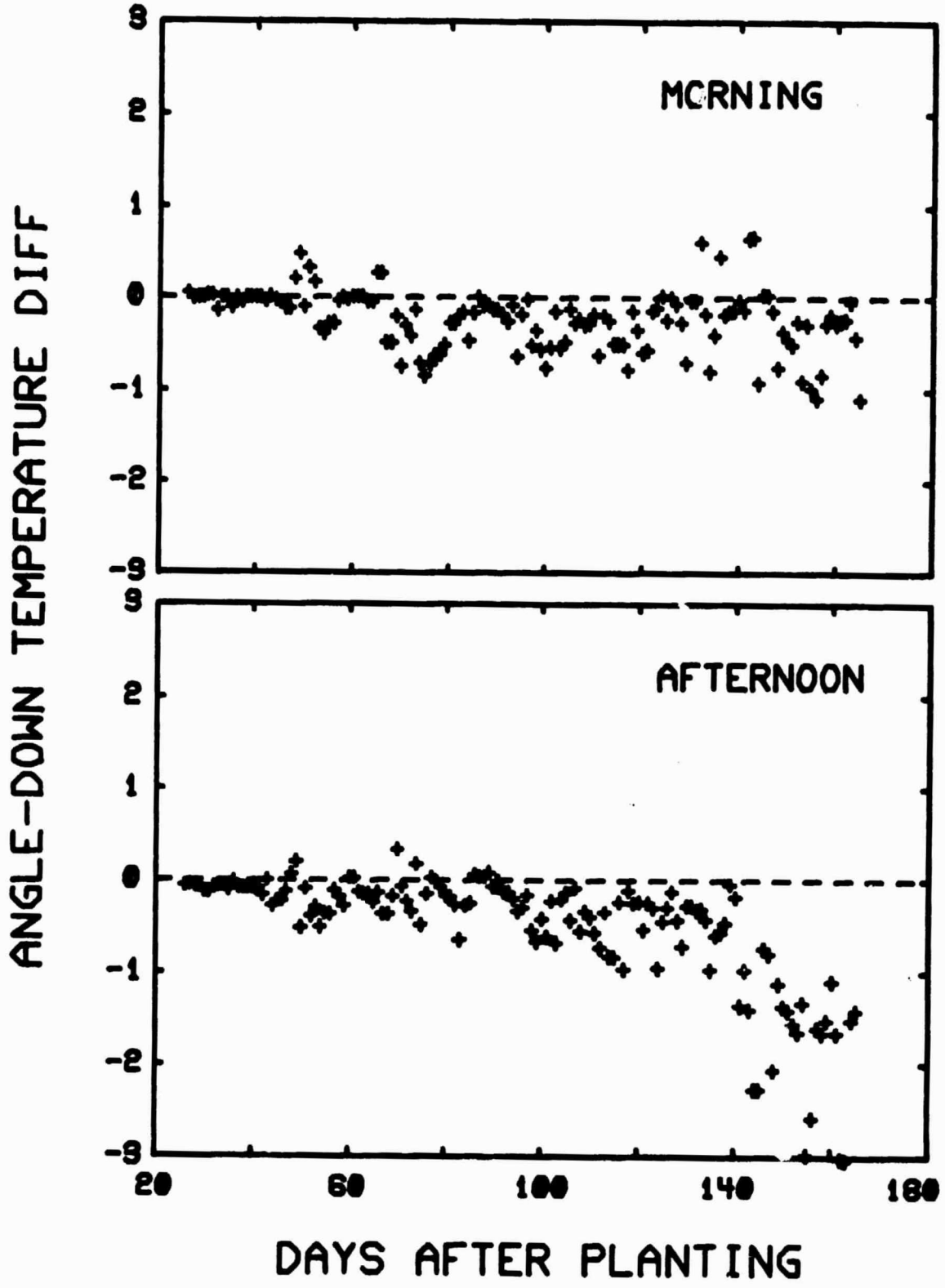

Figure 7. The temperature difference between measurements made holding the infrared thermometer at an angle of about 30° from horizontal and when holding the instrument vertically, as a function of days after planting.

is more pronounced for the afternoon measurements. After heading (about day 120 to 130) an angular measurement would be influenced more by heads than by leaves, whereas the nadir view would include mostly leaves. As the leaves senesce the nadir measurement would yield higher temperatures than from an angle. Until 140 days after planting, the angle-nadir temperatures differed by less than 1°C. Hatfield (1979) measured a maximum angle-nadir difference of -2°C when plants covered 20 to 50% of the ground.

An attempt was made to register ground and aircraft data. The exact pixel in which the ground data were acquired could not be identified in the airborne thermal imagery. The airborne data were therefore averaged over a 5 x 5 m pixel grid about the point where the ground sites were thought to be located. This time consuming procedure was done for seven flight days. The results are shown in Figure 8. Regression analysis yielded a near zero intercept (-.34) and a slope of 1.07, with an r^2 of 0.97.

A second comparison was made by averaging the aircraft pixel data over the entire field and averaging the nadir-looking ground data for the 16 sites. A total of 39 data sets were available for this purpose. The results are shown in Figure 9. Again, a near zero (0.15) intercept was obtained, as well as an identical slope (1.07) as the registered data in Figure 8.

These comparisons lend confidence that methods of detecting crop water stress and yield predictions developed from ground data can be

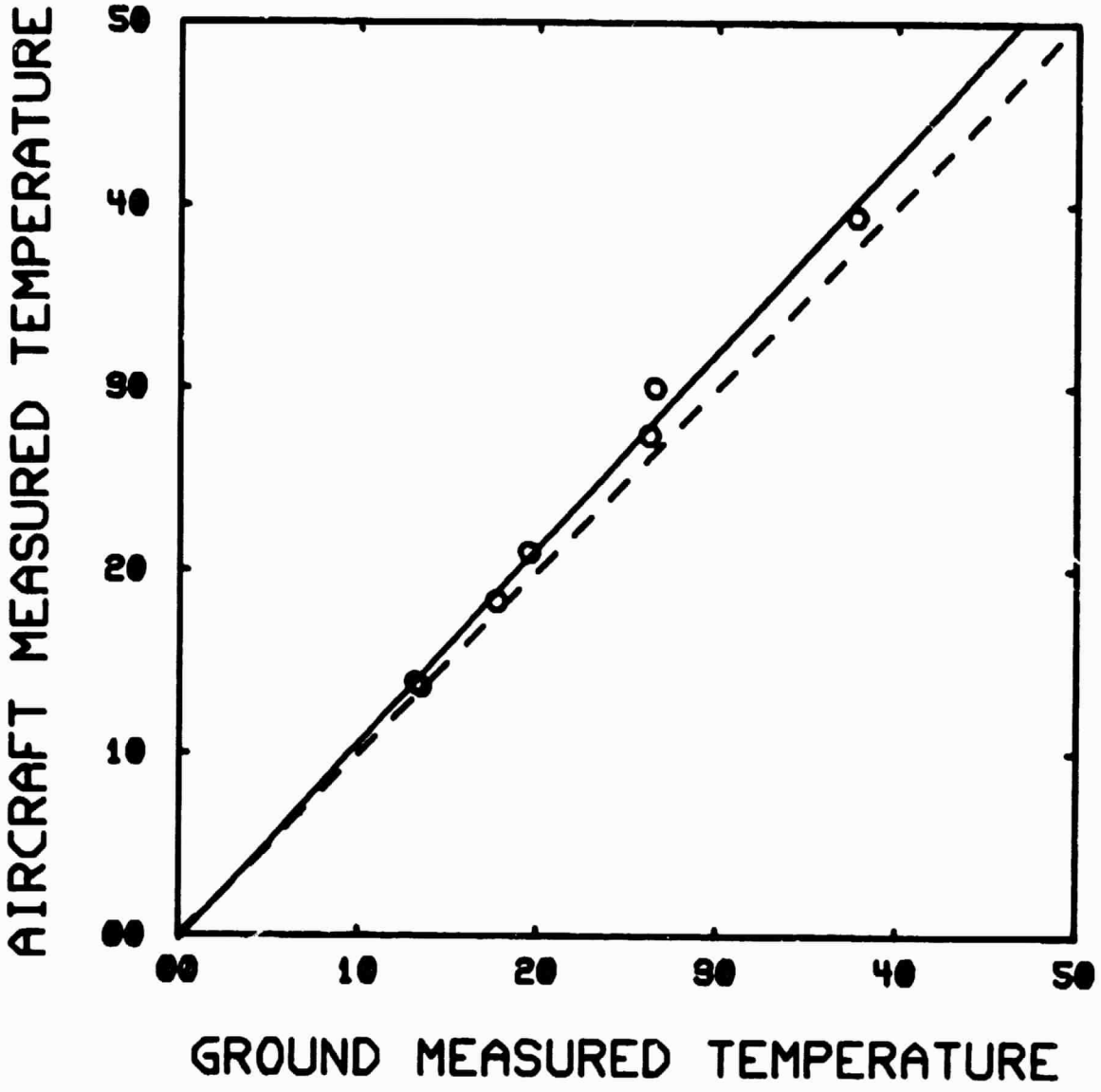

Figure 8. Aircraft versus ground (nadir) measured temperatures. Aircraft data were registered to the ground sites in time and space.

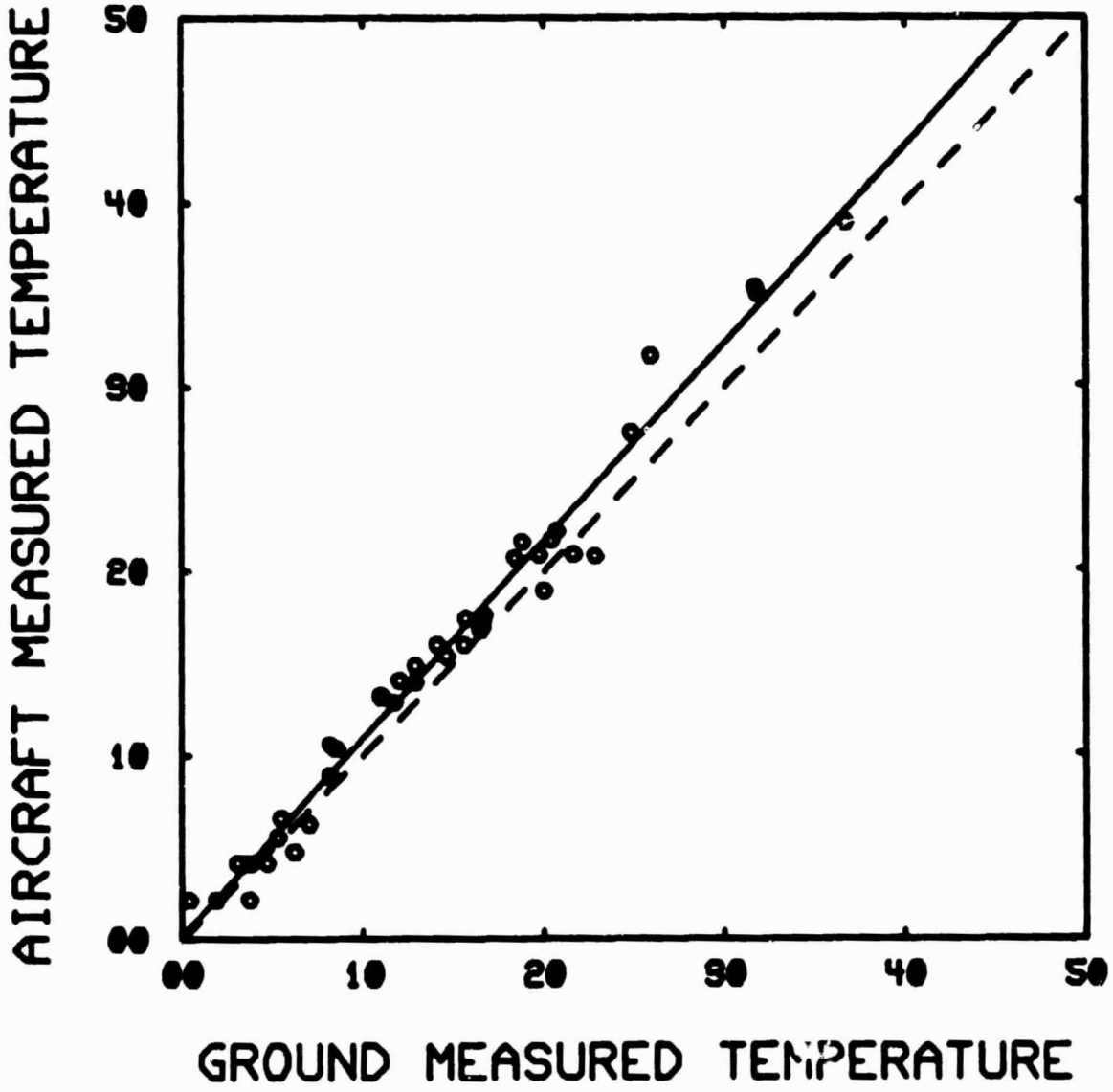

Figure 9. Aircraft versus ground (nadir) measured temperatures. Aircraft data were averaged over the entire field. Ground data are averages of the 16 sites.

extended to aircraft-derived data. The cause of the slope being greater than 1 may be due to inadequate calibration of the hand-held radiometer or possibly to an inexact atmospheric correction being applied to the aircraft-derived temperatures.

Spatial Integration of Aircraft-Measured Temperature

In the previous section we established that a good correlation exists between ground- and aircraft-acquired temperature data. To relate aircraft to satellite data requires that the aircraft data be spatially integrated. Data for the 1305 North-South flight of 16 May 1978 was used for an example. The 2 x 2 m pixels were averaged into four ha square blocks (200 x 200 m) and shown in Figure 10 (top). The maximum, minimum, mean, and standard deviation are given for each block. Temperatures varied from a high of 44.3° to a low of 21.2°C. The mean temperature varied from 29.5° to 33.3°C. Further integration into 16 ha blocks (400 x 400 m) yielded a mean value range of 30.1° to 32.9°C. Integrating to 64 ha blocks (800 x 800 m) changed the range of the mean only slightly (30.3° to 32.7°C) (Figure 11). Integrating the data to 256 ha (1600 x 1600 m), nearly the size of the field, yields a mean of 31.5°C. The mean temperature of the largest block (256 ha) was within ± 2°C from the highest and the lowest of the means of the 4 ha blocks.

The spatial variation of temperature that occurs in a undulating field is rapidly attenuated as the resolution of the instrument increases, as demonstrated in Figure 12. The symbols in Figure 12 represent the lowest and highest mean for each pixel size. The lines

Max = 36.2 Min = 26.3 Mean= 30.2 Sdev= 1.4	35.9 28.1 31.1 1.2	36.1 26.5 31.0 1.2	37.2 27.5 31.7 1.4	40.0 27.8 32.4 1.4	37.9 26.8 32.4 1.7	43.3 27.0 32.9 2.0	38.7 25.0 32.7 1.6
34.1 25.8 29.6 1.4	35.2 26.6 30.8 1.1	36.5 27.1 30.9 1.2	39.8 28.3 31.6 1.3	38.7 28.5 32.4 1.1	38.7 28.5 32.8 1.7	44.3 [illegible] 32.4 2.1	[illegible] 27.8 32.6 1.6
35.4 26.3 30.5 1.4	36.1 25.0 31.1 1.5	36.4 23.2 30.7 1.8	40.2 27.0 31.6 1.8	40.0 27.3 32.5 1.9	38.2 28.8 33.3 1.5	40.2 28.1 33.8 2.2	38.7 27.3 32.5 1.7
35.7 25.[illegible] 30.[illegible] 1.[illegible]	36.2 25.6 30.1 1.6	[illegible] [illegible] 30.[illegible] 2.0	37.2 23.5 31.1 1.7	36.5 27.3 32.0 1.4	39.0 27.3 33.0 1.9	38.5 27.0 32.7 1.7	40.8 25.6 32.6 2.0
33.6 26.0 30.2 0.9	34.4 26.0 30.9 1.4	36.0 21.2 29.7 2.0	35.3 25.0 30.[illegible] 1.3	36.7 25.5 31.0 2.2	38.2 27.1 32.1 1.7	37.2 28.3 32.3 1.4	37.5 28.1 32.1 1.3
33.7 27.1 30.1 0.8	[illegible] [illegible] 30.4 1.3	35.4 [illegible] 29.7 1.4	34.2 27.1 30.8 1.1	37.2 25.1 30.9 1.7	38.4 26.8 33.2 1.3	37.0 28.6 32.7 1.3	36.4 28.5 32.5 1.1
34.1 25.1 29.6 1.5	33.7 25.5 30.2 1.4	35.1 24.8 30.1 1.3	34.9 26.5 30.8 1.1	36.5 27.1 32.4 1.3	36.7 26.1 32.2 2.1	36.9 28.3 33.2 1.2	36.1 28.1 32.1 1.1
37.2 25.1 30.4 0.9	33.2 26.6 30.3 0.9	35.1 24.2 29.5 1.1	35.6 27.1 31.3 1.5	36.4 28.9 32.8 1.2	37.4 28.0 32.8 1.2	36.9 26.6 33.3 1.1	35.1 28.0 32.5 0.9

Max = 36.2 Min = 25.8 Mean= 30.4 Sdev= 1.4	39.8 26.5 31.3 1.4	40.0 26.8 32.5 1.5	44.3 25.0 32.7 1.9
36.2 25.0 30.3 1.4	40.2 22.8 30.9 1.9	40.0 26.6 32.7 1.8	40.8 25.6 32.9 2.0
34.4 26.0 30.4 1.2	38.0 21.2 30.2 1.6	38.4 25.1 32.0 2.0	37.5 27.3 32.4 1.3
37.2 25.1 30.1 1.3	[illegible] 24.2 30.4 1.5	37.4 26.1 32.6 1.5	36.9 26.6 32.7 1.2

Figure 10. Maximum, minimum, mean, and standard deviation for 2m x 2m pixels averaged to 200m x 200m (4ha) pixels (top) and averaged to 400m x 400m (16ha) pixels (bottom). Data for aircraft flight at 1305, 16 May 78.

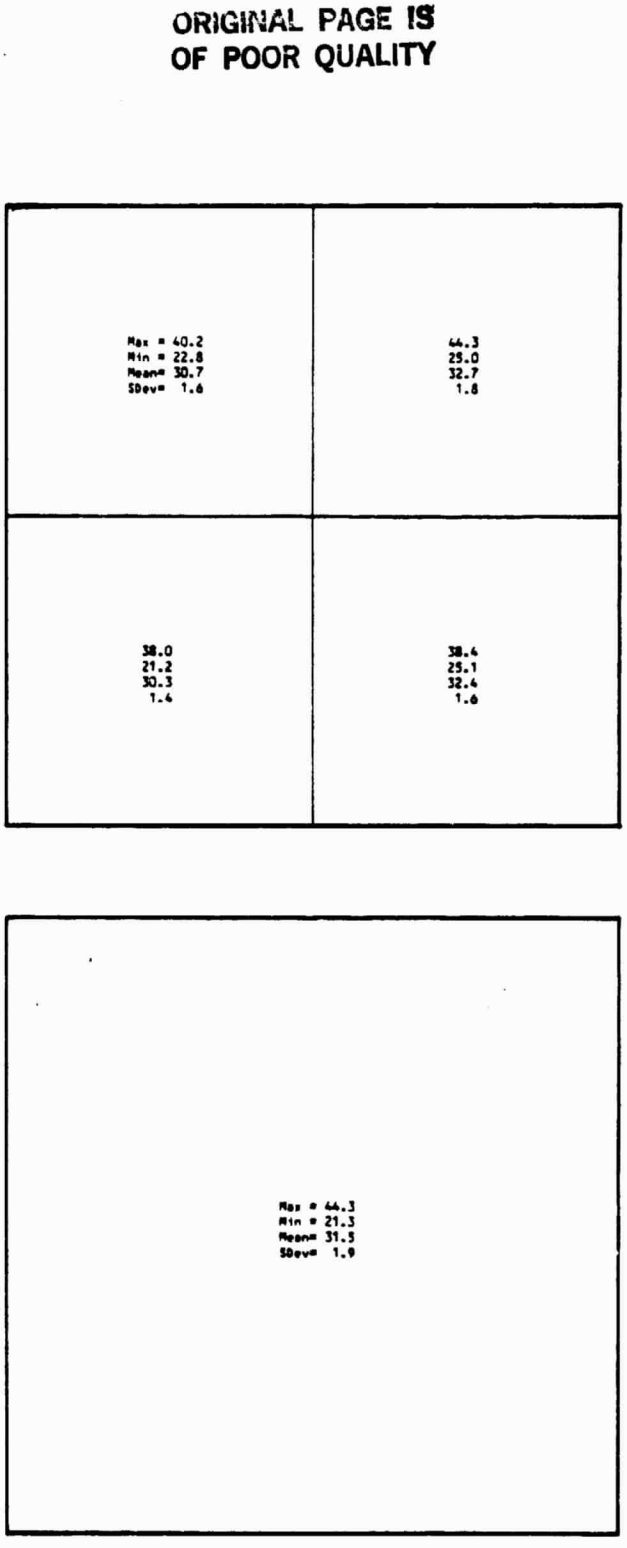

Figure 11. Maximum, minimum, mean, and standard deviation for 2m x 2m pixels averaged to 800m x 800m (64ha) pixels (top) and averaged to 1600m x 1600m (256ha) pixels (bottom). Data for aircraft flight at 1305, 16 May 78.

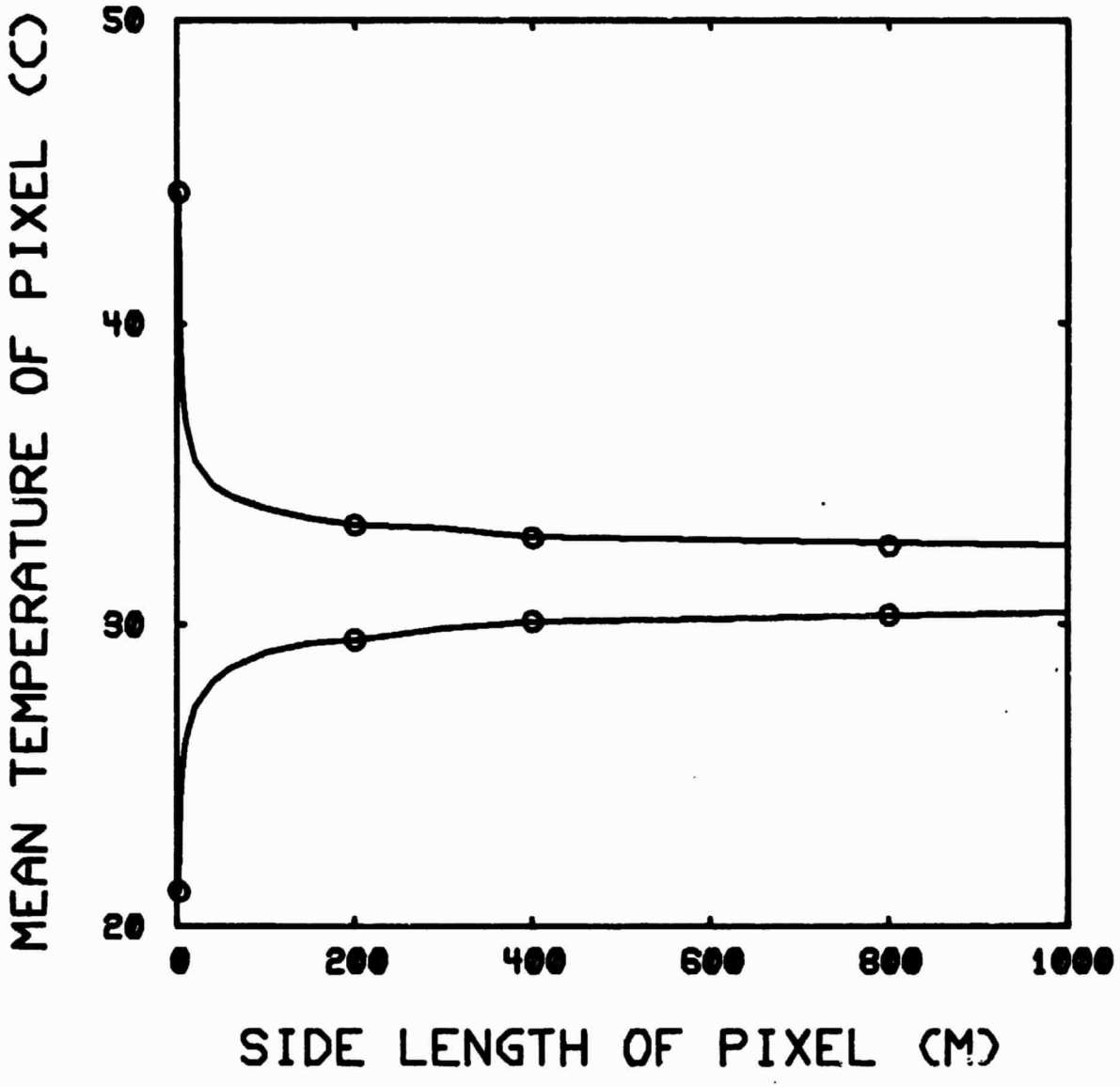

Figure 12. Mean temperature of pixels having the highest and lowest temperatures as a function of pixel size. Lines were drawn by interpolating plots of the mean temperature versus the logarithm of pixel side length.

were drawn by interpolating data from the plots of the mean pixel temperature and the logarithm of the pixel side length. Because of this interpolation, inferences about the data below 200 m side length are subject to question. With the length of the side of the resolution element of an HCMM pixel being 600 m, one can conclude that improving the resolution to 200 m would not significantly affect the estimation of the temperature within the field. Of course as the resolution improves below 200 m on a side, much more temperature detail becomes evident. Millard, Geottelman, and LeRoy (1981) reached the same conclusion from a different analysis of these data.

Aircraft and Spacecraft Derived Imagery

Figures 13, 14, and 15 are images obtained from the low altitude aircraft data for the afternoon of 16 May 1978 and for the morning and afternoon of 20 May 1978. Imagery is available for other dates, but these were selected to correspond with HCMM data to be shown in subsequent figures. The three figures clearly show the temperature inhomogeneity that occurs in undulating terrain. The northeast section of the field is the most rugged, and the imagery shows that the temperature extremes occurred there. The morning image (Figure 14) shows a more uniform temperature distribution (note the expanded temperature scale). Temperature extremes differed by about 4°C. Figure 15 shows imagery for the afternoon of 20 May 1978. In general, surface temperatures were much warmer on 20 May than on 16 May. Temperatures were averaged over all pixels in the field for each image and the 20 May temperature was 7.5°C warmer than on 16 May.

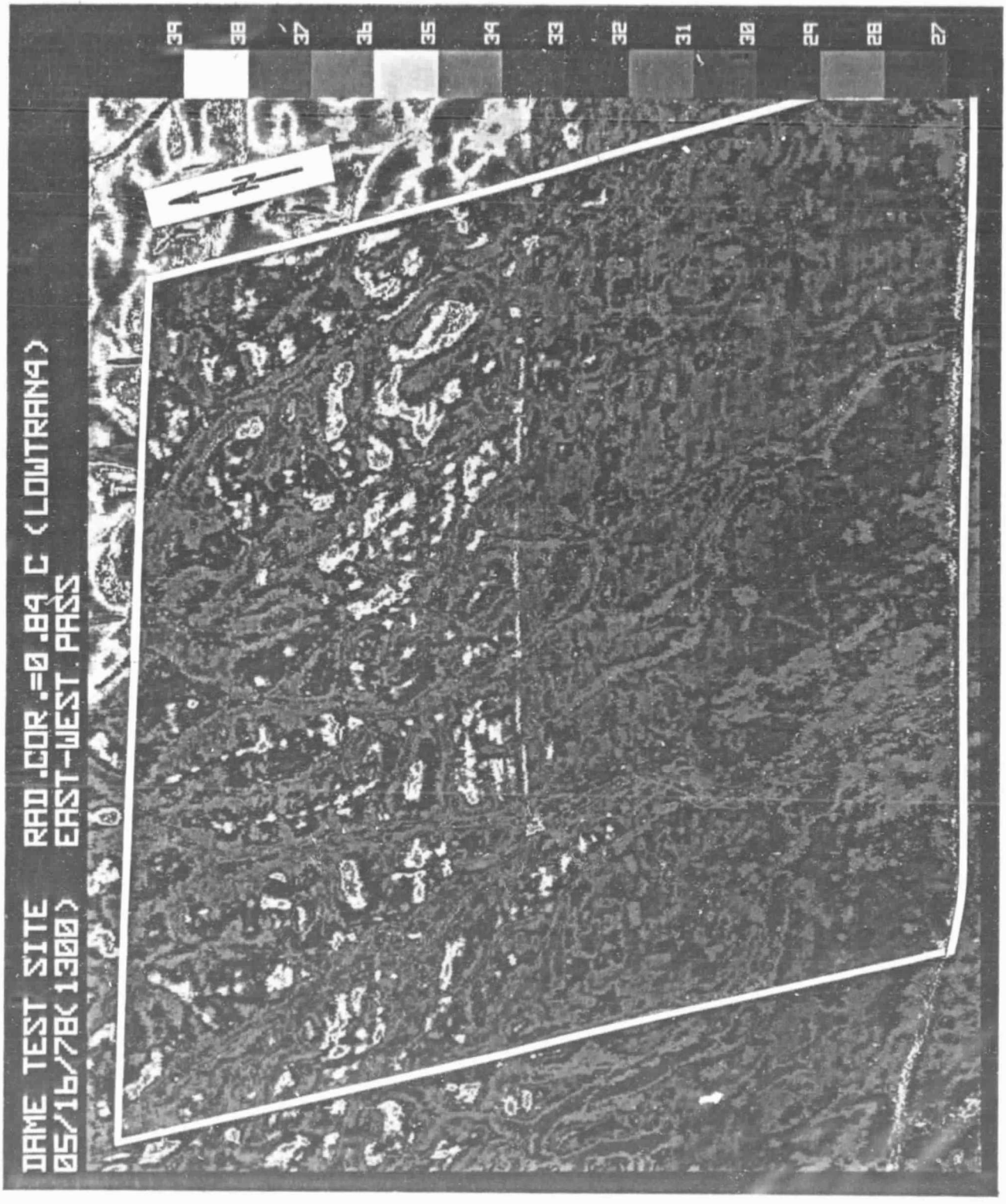

Figure 13. Temperature image of the Dunnigan agro-meteorological experiment test field for 16 May 1978, in conjunction with a U-2 and HCMM overpass, approximate pixel size 2m x 2m.

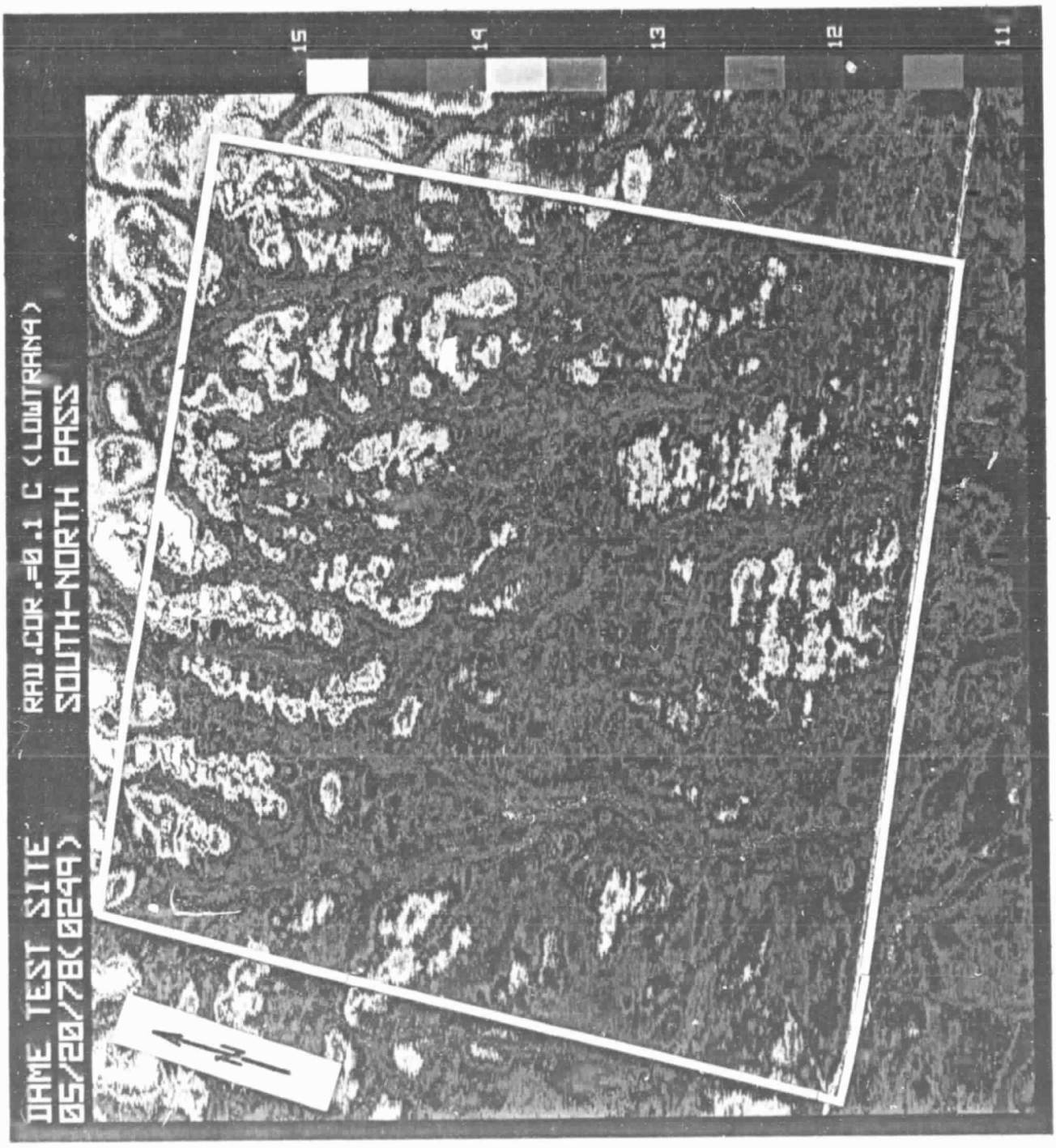

Figure 14. Temperature image of the field obtained at 0249, 20 May 1978, in conjunction with an HCMM overpass, approximate pixel size 2m x 2m.

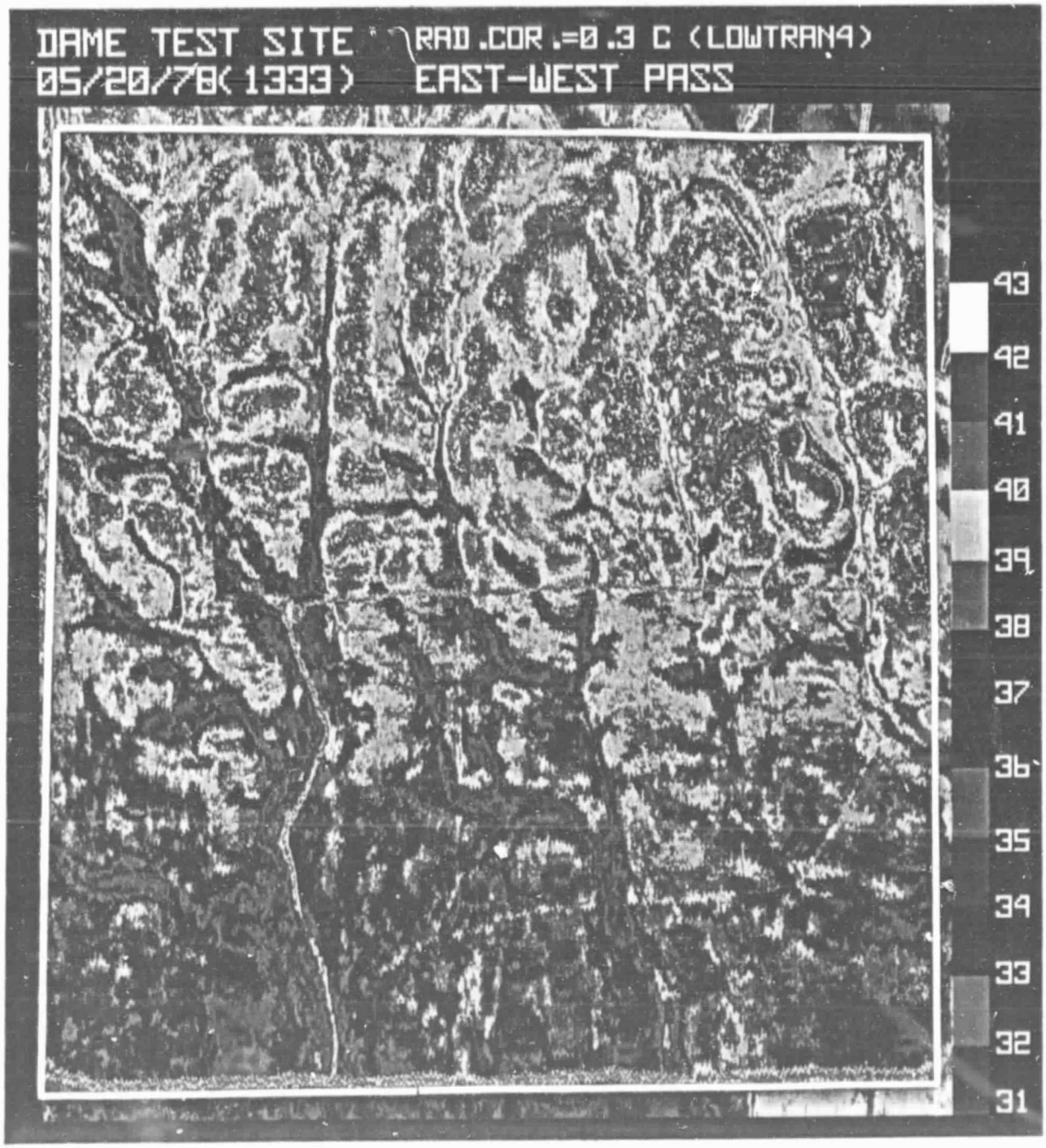

Figure 15. Temperature image of the field at 1333, 20 May 1978, in conjunction with an HCMM overpass, approximate pixel size 2m x 2m.

In Figures 2, 13, and 15, the field boundaries in the upper right hand corner are quite distinct. The area outside these boundaries was not planted to a crop. Weeds and grasses were present because of the abundant rainfall. Comparing this area with the area inside the field boundaries indicates that the weeds and grasses were nearly the same temperature on 16 and 20 May. The large change of temperature within the field was due to ripening of the barley and the senescence of the leaves. This demonstrates that surface temperatures can be used to discriminate ripening.

A U-2 derived image for the afternoon of 16 May 78 is shown as Figure 16. Temperatures within the field ranged from 30° to 34°C. This is well within the range of low altitude aircraft-derived temperatures (Figure 12). The U-2 pixel was about 70 m side length. The temperature range for this pixel supports the interpolated data shown in Figure 12. Thus we can extend an earlier observation that, for fields of this type (i.e., undulating terrain planted to the same crop), pixel sizes 70 m x 70 m and larger yield essentially the same temperature range.

HCMM imagery at nearly the same time as the aircraft data are shown in Figures 17, 18, and 19. Location of the site was extremely difficult and we are not completely confident that the nine pixels used were totally within the field. Another complication was the calibration of the HCMM radiometer. Barnes and Price (1980) reported the pre-launch calibration, and also a post-launch calibration over a lake in New Mexico. The post-launch values were about 5.5°C below the pre-launch

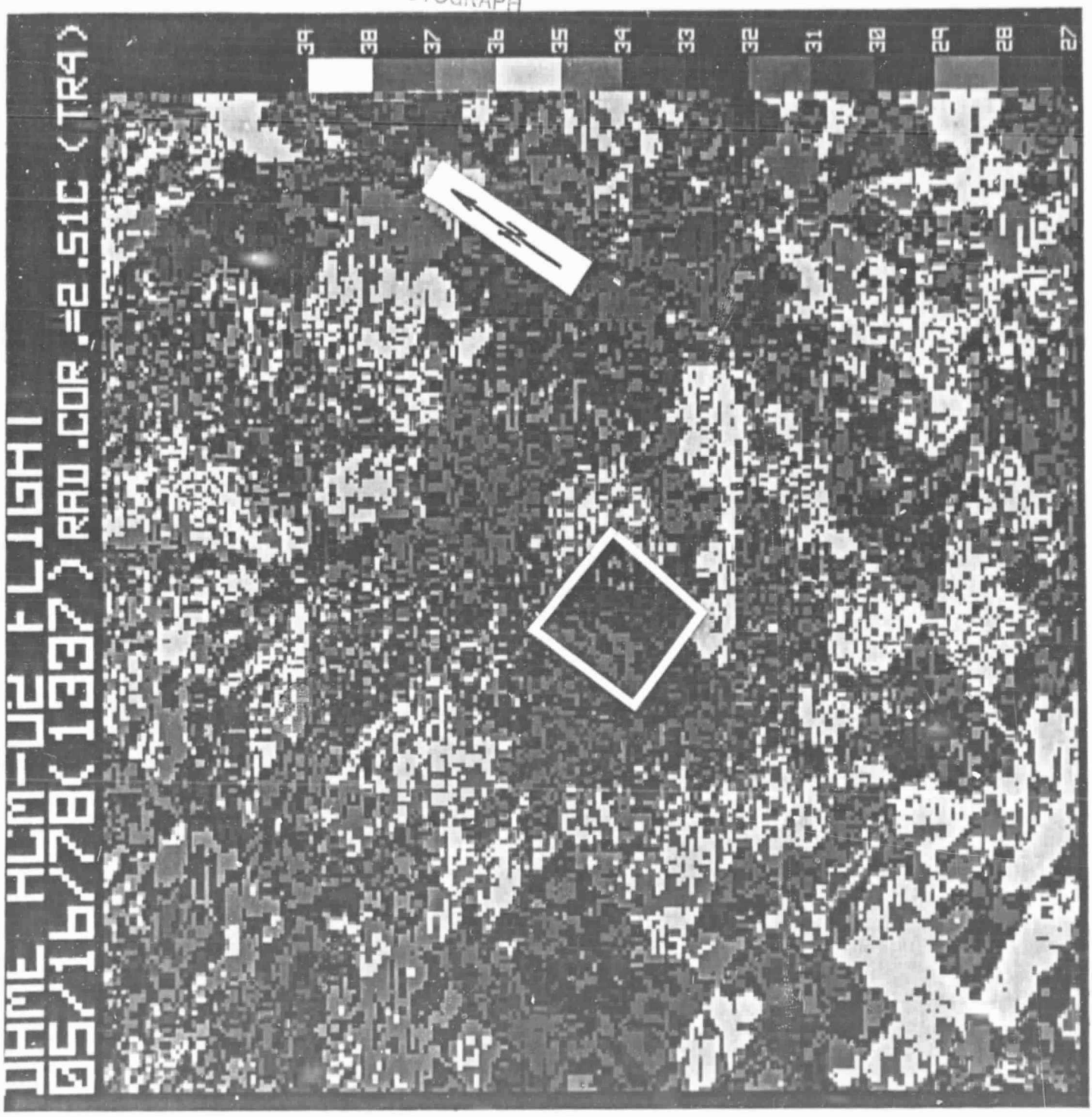

Figure 16. Temperature image of the field at 1337, 16 May 1978, obtained with the U-2, approximate pixel size 70m x 70m.

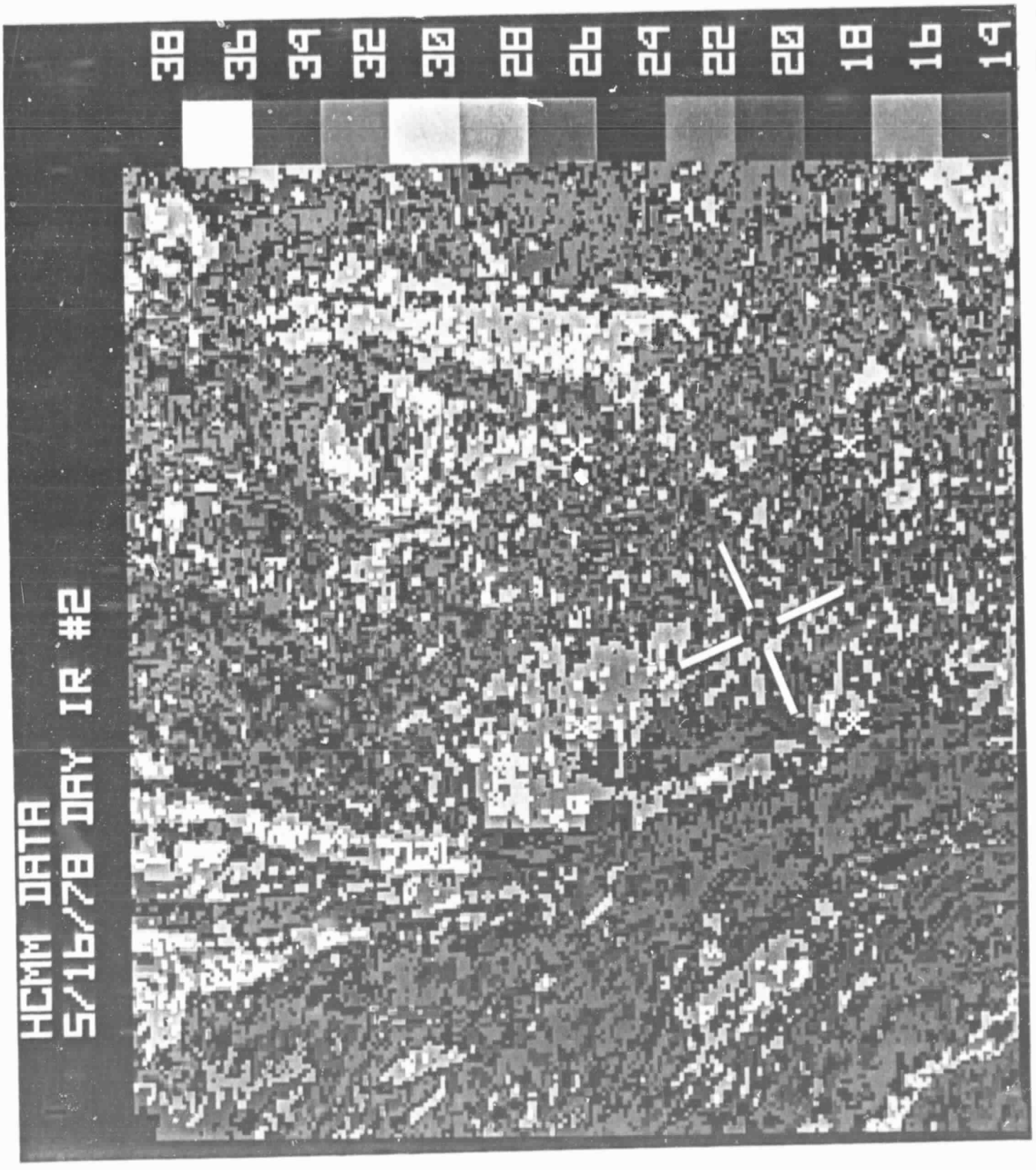

Figure 17. Temperature image obtained with HCMM satellite at approximately 1330, 16 May 1978, approximate pixel size 600m x 600m.

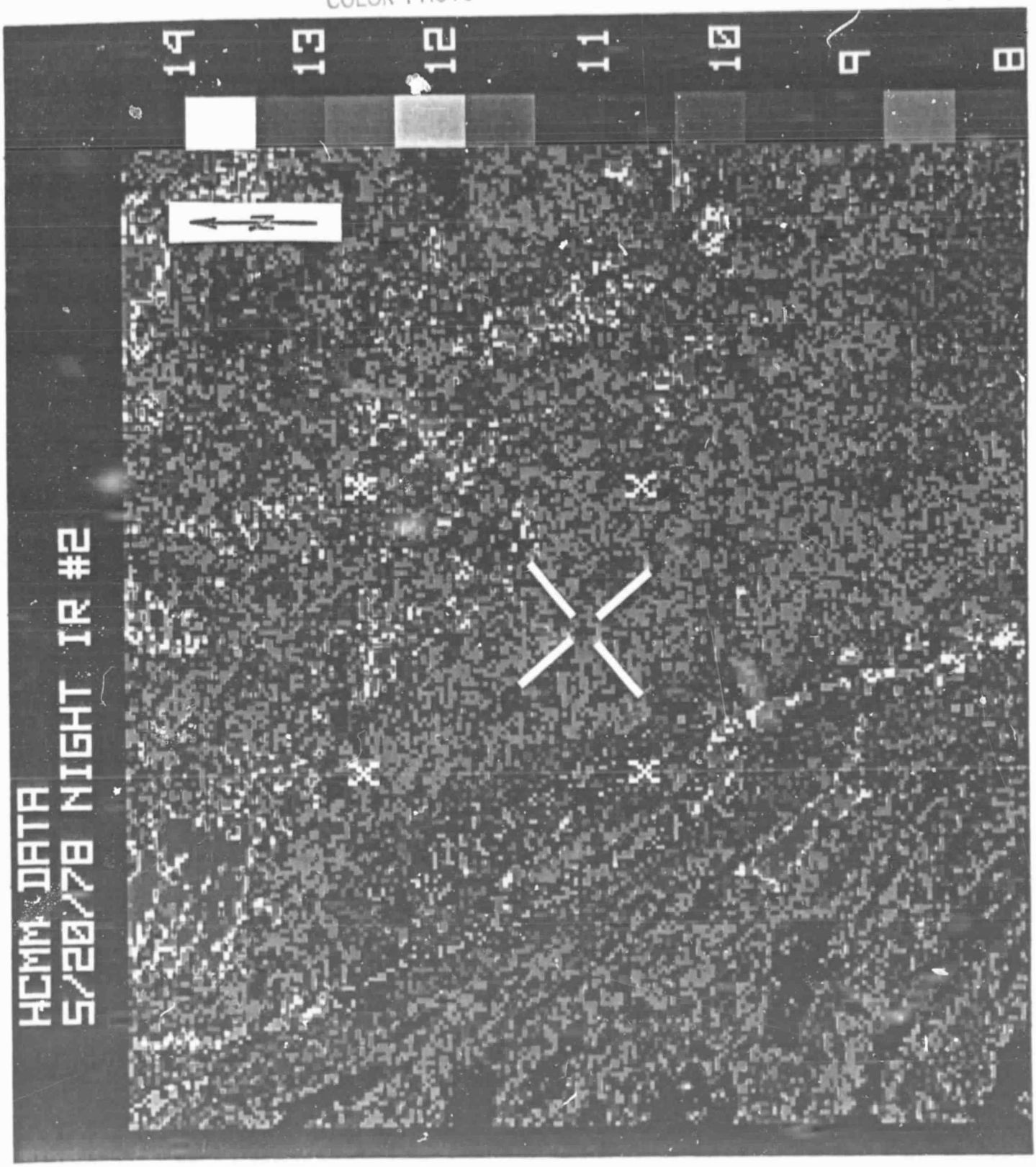

Figure 18. Temperature image obtained with the HCMM satellite at approximately 0230, 20 May 1978, approximate pixel size 600m x 600m.

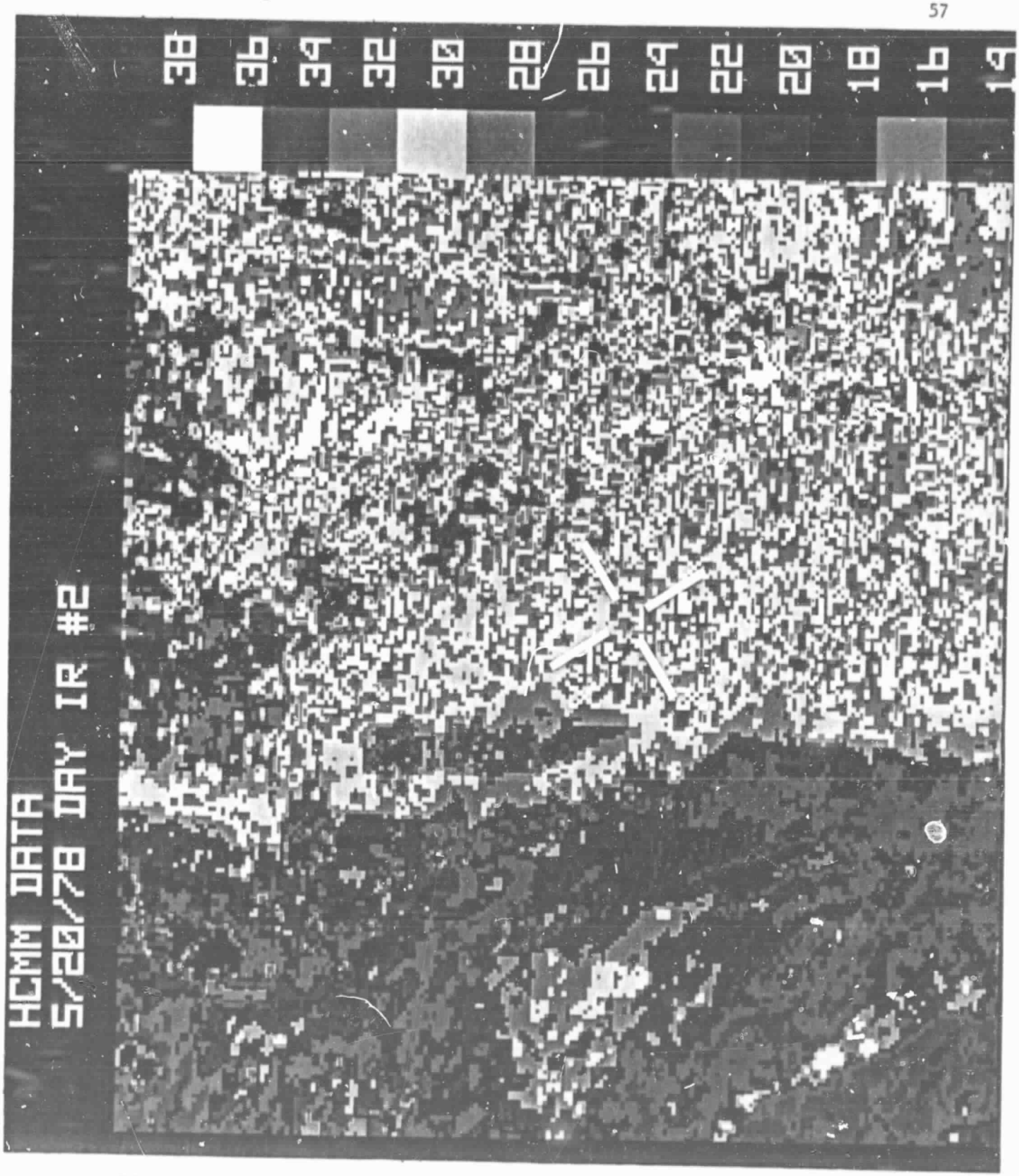

Figure 19. Temperature image obtained with the HCMM satellite at approximately 1330, 20 May 1978, approximate pixel size 600m x 600m.

values. Figures 17-19 are in terms of the post-launch calibration. We obtained temperature values from where we believe the field was located. These data are compared with the aircraft data in Figure 20. The post-launch data fall well below the aircraft data. When 5.5°C is added to the HCMM values, they fall much closer to those from the aircraft. Three data points are not sufficient to calibrate the HCMM data with the aircraft data but they are sufficient to show that the pre-launch calibration was superior to the post-launch one. It is possible that the atmospheric correction applied to the HCMM data was too high at night and too low during the day. The U-2 value falls nearly on the 1:1 line.

CONCLUSIONS

A crop water stress index was developed from energy balance considerations to quantify the effect of stress on plants by using remotely sensed canopy temperatures.

Aircraft derived surface temperatures are well correlated with ground based temperature measurements. Thus, ground-based measurements can be economically used to develop strategies for soil moisture and crop water stress evaluations that can be readily adapted to aircraft derived data.

Integrating aircraft derived data from 2 m x 2 m pixels to 200 m x 200 m pixels removed spatial variation of temperature to the point that further integration to 800 m x 800 m pixels showed essentially the same temperature detail. U-2 data indicate that pixels greater than 70 m x 70 m yield results similar to the 200 m x 200 m pixel. These results

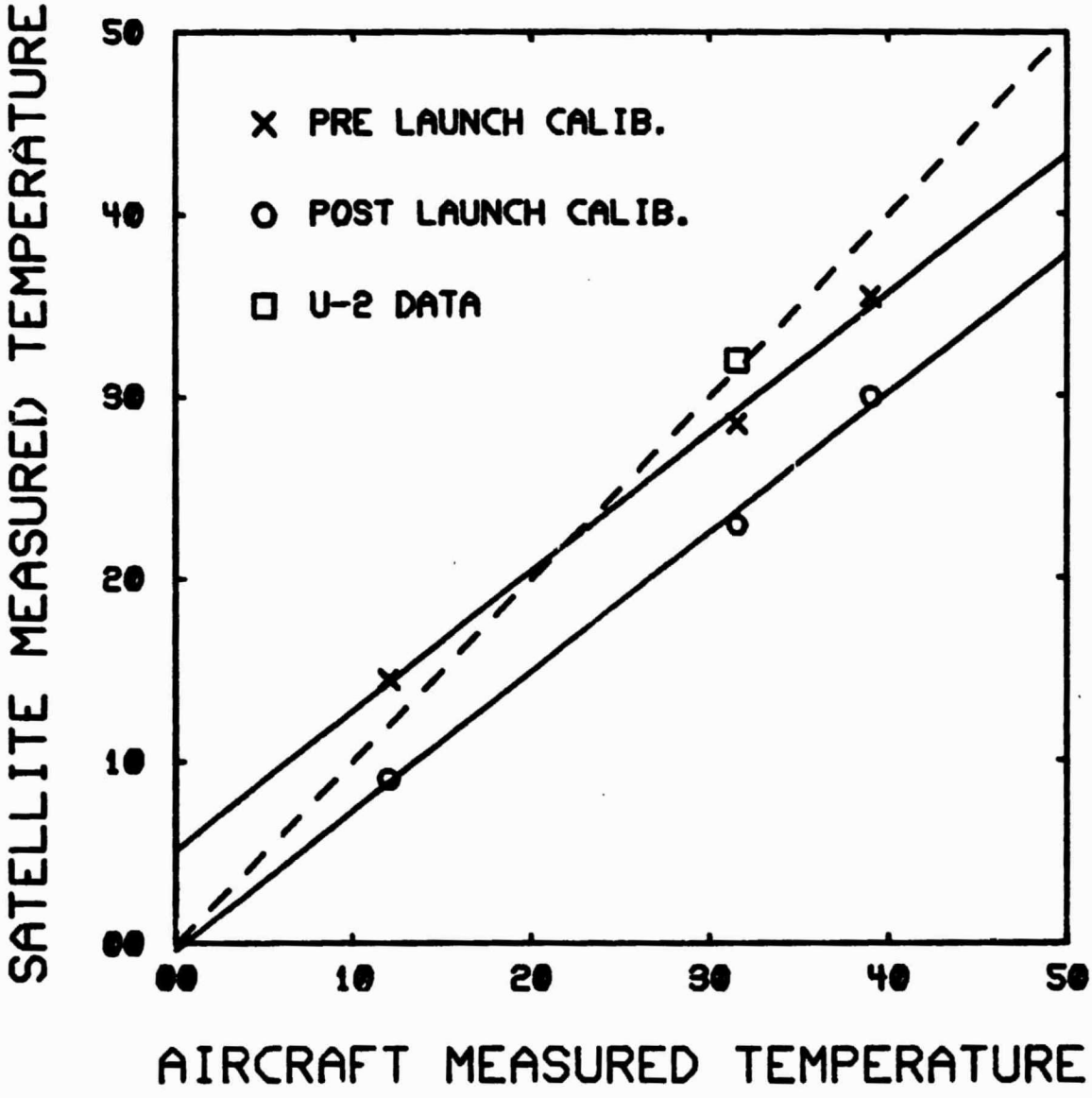

Figure 20. Satellite versus aircraft measured surface temperatures. The square symbol indicates the U-2 derived temperatures. The x's and circles represent HCMM data using the pre- and post-launch calibrations, respectively.

suggest that there is little advantage to decreasing pixel size from 800 m x 800 m to 70 m x 70 m as far as assessing temperatures over undulating terrain is concerned. The smaller pixels, however, would make it much easier to locate specific areas only 9 large pixels in size.

The pre-launch calibration of the HCMM radiometer yielded temperatures closer to aircraft derived temperatures than did the post-launch calibration. Using the pre-launch calibration, temperatures were higher at night and lower during the day than were the aircraft temperatures. This raises a question as to the calibration of the HCMM radiometer or to the adequacy of regionally acquired radiosonde data used in conjunction with algorithms to adjust for atmospheric effects.

Intensive ground and aircraft experiments that are geared to the growth and development of plants should not be committed in conjunction with a satellite program until the satellite is launched and is operational. All biological field experiments are subject to the extremes of nature.

REFERENCES

Barnes, W. L. and J. C. Price. Calibration of a satellite IR radiometer. Applied Optics, 19: 2153-2161, 1980.

Hatfield, J. L. Canopy temperatures: the usefulness and reliability of remote measurements. Agron. J. 71:889-892.

Howell, T. A., W. R. Jordan, and E. A. Hiler. Evaporative demand as a plant stress. In Modification of the aerial environment of plants, Barfield, B. J. and J. F. Gerber, eds. ASAE Mono. No. 2, St. Joseph, MI, 97-113, 1979.

Idso, S. B., R. D. Jackson, and R. J. Reginato. Compensating for environmental variability in the thermal inertia approach to remote sensing of soil moisture. J. Applied Met., 15: 811-817, 1976.

Idso, S. B., R. D. Jackson, and R. J. Reginato. Remote sensing of crop yields. Science, 196: 19-25, 1977.

Idso, S. B., T. J. Schmugge, R. D. Jackson, and R. J. Reginato. The utility of surface temperature measurements for the remote sensing of surface soil water status. J. Geophys. Res., 80: 3044-3049, 1975.

Idso, S. B., R. D. Jackson, P. J. Pinter, Jr., R. J. Reginato, and J. L. Hatfield. Normalizing the stress-degree-day parameter for environmental variability. Agric. Met., 1981 (in press).

Jackson, R. D., R. J. Reginato, and S. B. Idso. Timing of ground truth acquisition during remote assessment of soil water content. Remote Sensing of Environment, 4:249-255, 1976.

Jackson, R. D., R. J. Reginato, and S. B. Idso. Wheat canopy temperature: a practical tool for evaluating water requirements. Water Resources Res., 13: 651-656, 1977.

Jackson, R. D., S. B. Idso, R. J. Reginato, and P. J. Pinter, Jr. Canopy temperature as a crop water stress indicator. Water Resources Res., 1981 (in press).

Jensen, M. E., ed. Consumptive use of water and irrigation water requirements. Irrigation and Drainage Div., ASCE, 215 p., 1974.

Millard, J. P., R. C. Goettelman, and M. J. LeRoy. Infrared-temperature variability in a large agricultural field. Intern. J. of Remote Sensing, 1981 (in press).

Millard, J. P., J. L. Hatfield, and R. C. Goettelman. Equivalence of airborne and ground-acquired wheat canopy temperatures. Remote Sensing of Environment, 8: 273-275, 1979.

Millard, J. P., R. J. Reginato, R. C. Goettelman, S. B. Idso, R. D. Jackson, and M. J. LeRoy. Experimental relations between airborne and ground-measured wheat canopy temperatures. Photogram. Eng. and Remote Sensing, 46: 221-224, 1980.

Monteith, J. L. Principles of environmental physics. Edward Arnold, Ltd., London, 241 p., 1973.

Reginato, R. J., S. B. Idso, J. F. Vedder, R. D. Jackson, M. B. Blanchard, and R. C. Goettelman. Soil water content and evaporation determined by thermal parameters obtained from ground-based and remote measurements. J. Geophys. Res., 81: 1617-1620, 1976.

Russell, G. Crop evaporation, surface resistance and soil water status. Agric. Met., 21: 213-226, 1980.

Szeicz, G. and I. F. Long. Surface resistance of crop canopies. Water Resources Res., 5: 622-633, 1969.

Thom, A. S. and H. R. Oliver. On Penman's equation for estimating regional evaporation. Quart. J. R. Met. Soc., 103: 345-357, 1977.

Van Bavel, C. H. M. Changes in canopy resistance to water loss from alfalfa induced by soil water depletion. Agric. Met., 4: 165-176, 1967.

Van Bavel, C. H. M. and W. L. Ehrler. Water loss from a sorghum field and stomatal control. Agron. J., 60: 84-86, 1968.

Whitman, C. E. The effects of topoclimate on the growth and yield of barley in northern California. M.S. thesis, Univ. of California Davis, 123 p., June 1981.